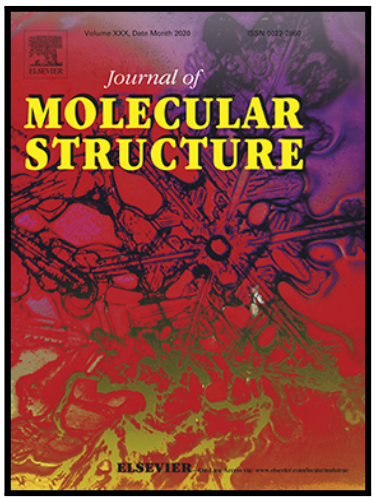

Novel isoniazid-spirooxindole derivatives: design, synthesis, biological evaluation, in silico ADMET prediction and computational studies

Mayuri A. Borad , Divya J. Jethava , Manoj N. Bhoi , Chirag N. Patel , Himanshu A. Pandya , Hitesh D. Patel

PII: S0022-2860(20)31206-0
DOI: https://doi.org/10.1016/j.molstruc.2020.128881
Reference: MOLSTR 128881

To appear in: *Journal of Molecular Structure*

Received date: 11 May 2020
Revised date: 1 July 2020
Accepted date: 9 July 2020

Please cite this article as: Mayuri A. Borad , Divya J. Jethava , Manoj N. Bhoi , Chirag N. Patel , Himanshu A. Pandya , Hitesh D. Patel , Novel isoniazid-spirooxindole derivatives: design, synthesis, biological evaluation, in silico ADMET prediction and computational studies, *Journal of Molecular Structure* (2020), doi: https://doi.org/10.1016/j.molstruc.2020.128881

Highlights:

- Novel isoniazid containing spirooxindole derivatives were synthesized as potential anti-mycobacterial agent.
- Compound **6ab** proves to be best anti-mycobacterial agent against H_{37}Rv strain and MDR-TB.
- The synthesized molecules docked with isoniazid-resistant I21V enoyl-ACP(COA) reductase mutant enzyme from *Mycobacterium tuberculosis* in Complex with NADH-INH (PDB entry: 2IE0).
- Molecular dynamics study for the structural integrity and stability of the complex.
- In silico ADMET prediction of synthesized compounds for good pharmacokinetic properties.

Novel isoniazid-spirooxindole derivatives: design, synthesis, biological evaluation, *in silico* ADMET prediction and computational studies

Mayuri A. Borad[a], Divya J. Jethava[a], Manoj N. Bhoi[a*], Chirag N. Patel[b], Himanshu A. Pandya[b], and Hitesh D. Patel[a*]

[a]Department of Chemistry, School of Sciences, Gujarat University, Ahmedabad, India.

[b]Department of Bioinformatics, Applied Botany Centre (ABC), School of Sciences, Gujarat University, Ahmedabad 380009, Gujarat, India

E-mail: mayuri.borad@gmail.com, divyajethva187@gmail.com, manoj18bhoi@gmail.com, hitesh13chem@rediffmail.com Tel.: +91-079-26300969; fax: +91-079-26308545.

Abstract

In the present scenario, the Synthesis of new and desired antimycobacterial agent has an eternal demand to resist *Mycobacterium tuberculosis (MTB).* The design and identification of new molecules for the treatment of tuberculosis is an important task in organic as well as medicinal chemistry research. In the present study, we have reported the combination of the desired compound using two versatile and significant moieties, isoniazid and spirooxindole derivatives. A series of novel isoniazid-spirooxindole hybrid molecules (**6a-6ao)** were designed, synthesized, and well-characterized by various spectroscopic methods. We have evaluated for their *in vitro* antimycobacterial activity against *Mycobacterium tuberculosis* $H_{37}Rv$ (MTB) strain and MDR-TB. Among them, Compound **6ab** was found to be the most effective compare to other compounds. ADMET-related descriptors were to be calculated of all the compounds to predict the pharmacokinetic properties for the selection of the effective and bioavailable compounds. In addition, molecular docking and molecular dynamics studies reveal that the binding modes of all the compounds in the active site of isoniazid-resistant enoyl-ACP(COA) reductase, which helped to establish a structural basis of inhibition of Mycobacterium tuberculosis.

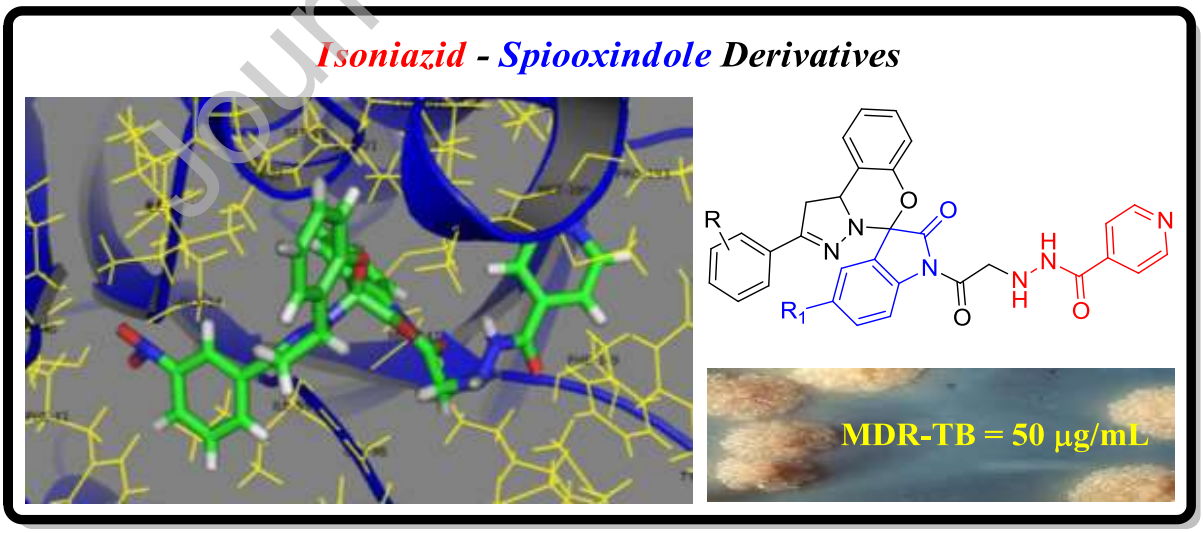

Keywords: ADMET properties, Antimycobacterial activity, Isatin, Isoniazid-spirooxindole, Molecular docking, Molecular dynamics

1. Introduction

Microbial infections are a growing problem in contemporary medicine, yet only a few antimicrobial agents are used in clinical practice. *Mycobacterium tuberculosis* (MTB) is a pathogenic bacterial species in the genus *Mycobacterium* and the causative agent of most cases of tuberculosis (TB).[1] It typically affects the lungs (pulmonary TB) but can affect other sites as well (extra-pulmonary TB). The disease is spread in the air when people who are sick with pulmonary TB expel bacteria, for example by coughing. Overall, a relatively small proportion (5-15%) of the estimated 2-3 billion people infected with *M. tuberculosis* will develop TB disease during their lifetime. However, the probability of developing TB is much higher among people infected with HIV.[2] As stated by the World Health Organization (WHO) Global Tuberculosis Report 2015, Around 9.6 million people are estimated to have tumbled ill with TB, and 1.5 million people deaths from the disease were reported in 2014.[3] Keeping insight into the above statistics, WHO declared TB as a global health emergency and aimed at saving 14 million lives between 2006 and 2015.[4] Streptomycin, Isoniazid, Rifampin, Ethambutol, and Pyrazinamide are the first-line drugs for TB control while, second-line drugs for treatments are *p*-aminosalicylic acid, Ethionamide, Cycloserine, macrolide antibiotics, such as Azithromycin, Fluoroquinolones, etc.. There was an extreme deterioration in the number of TB cases, after the discovery of many effective anti-TB drugs during the 1950s and 1970s. But, due to the emergence of multi-drug resistant tuberculosis (MDR-TB), drug-resistant tuberculosis (XDR-TB) and totally drug-resistant tuberculosis (TDR-TB), the number of TB cases has been increasing rapidly throughout the world since the 1980s.[5] The main problem accompanying antimycobacterial drugs is poor compliance with prolonged treatment and regimens used to treat TB that is badly tolerated, relatively ineffective, expensive, and must be taken for at least 2 years.[6] So, there is an exigent need for new anti-tuberculosis drugs that are active towards the broad spectrum of species of the *Mycobacterium* genus become obvious.

A number of anti-tubercular (anti-TB) drugs (Fig. 1) have been established over the past decades. However, the drug-resistance issue has not been resolved as yet. Thus, there is a tremendous need to develop new anti-TB drugs that are active against both acute and chronic growth phases of mycobacterium to stop all forms of drug resistant-TB.[7] In recent years several, new drug candidates or repurposed drugs namely linezolid, TMC207, Moxifloxacin, OPC67683, PA824, Gatifloxacin, Rifapentine, PNU100480, AZD5847, SQ109, etc.[8] have been still developed and some of them are also in the improvement stages of clinical trials for the treatment of tuberculosis.[9,10] Among them, only one drug that is bedaquiline has been recently approved by the FDA for its use in drug-resistant tuberculosis.[11]

Due to the global impact of this infectious disease, a great deal of research work is being devoted to recognizing newer molecular entities that are dynamic against the microbial strains. Several different approaches such as molecular alterations of the known drugs in combinatorial

chemistry, targeting bacterial virulence, structure-based drug discovery, high-throughput screening have been discovered to search innovative and novel biologically important molecules.[12,13] The molecular modification approach has been found to be very promising, among all these strategies. Several drugs that are available in the market have been developed by using this strategy. The main aim of molecular modification is to do chemical change in a molecule for the enhancement of its pharmaceutical, pharmacokinetics or pharmacodynamics properties.

Isoniazid (INH) has been widely used as a frontline anti-tubercular drug for the treatment of TB for the past 40 years.[14] It is a prodrug and must be activated by bacterial catalase. It is activated by catalase-peroxidase hemoproteins, KatG, which couples the isonicotinic acyl with nicotinamide adenine dinucleotide (NADH) to form the isonicotinic acyl-NADH complex [15], that binds with the enoyl-acyl carrier protein (ACP) reductase InhA, which is involved during the mycolic acid synthesis.[16] INH inhibits the synthesis of mycolic acid which is required for the mycobacterial cell wall. It is metabolized in the liver to form compounds such as hydrazine, which is toxic to the central nervous system and other body organs.[17] Recent reports indicate that the incorporation of hydrophobic moieties into the basic structure of INH increases penetration of the drug into the highly lipophilic cell wall of the bacterium. Several researchers have introduced the amidoether functionality into biologically active molecules and the resulting hybrids exhibited good biological activities.[18,19] Additionally**,** spirocyclic scaffolds are being progressively utilized in drug discovery. The construction of a spiro heterocyclic framework has always been a challenging endeavor for synthetic organic chemists as it frequently requires synthetic design based on specific strategies. Spiro cyclic building blocks have been subjected to make more pharmaceutically active molecules. Spirooxindole and its derivatives have attracted considerable interest to researchers in the area of synthetic organic chemistry as well as medicinal chemistry because they are present in many natural products and exhibits highly noticeable biological activities.[20, 21] It has been reported that the sharing of the C-3 atom for the synthesis of spirooxindoline derivatives can highly enhance biological activity.[22] Amongst them, some of the spirooxindoles derivatives are recognized for their antimycobacterial properties and have been shown comparable or even better activities than some of the first-line TB drugs. [23,24]

Inspiration from the previous studies and in continuation of our efforts towards the synthesis of new anti-tuberculosis agents, we have here reported spirooxindole derivatives linkage with isoniazid drug to form a new series of isoniazid-spirooxindole derivatives. All the derivatives were synthesized and well-characterized with various spectroscopic techniques. The synthesized compounds were screened for their *in vitro* antimycobacterial activity against *Mycobacterium tuberculosis* $H_{37}Rv$ (MTB) and also against MDR-TB. Additionally, we have carried out computational studies such as molecular docking, molecular dynamics, and *in silico* ADMET prediction of our compounds.

2. Materials and methods

2.1. Chemistry

All Starting materials and other reagents were purchased from commercial suppliers (Merk, sigma Aldrich, Avra, spectrochem, etc.) and were used without any further purification unless otherwise indicated. The reactions were examined by thin-layer chromatography (TLC) and terminated as arbitrated by the consumption of starting material. TLC was performed on silica gel G 60 F254 (Merck) plate. It was visualized by UV radiation or exposure to iodine vapors. Gravitational column chromatography was conducted over silica gel 60 (60-120 µm). CEM Discover microwave system (model no.: 908010; make up CEM Matthews. Inc, USA) was used for synthesis. The nomenclature of the compounds was performed using CambridgeSoft.ChemOffice.2010. v12. The melting points were recorded on an optimelt automated melting point system that was uncorrected. IR spectra were recorded at room temperature in the region from 500-3950 (cm^{-1}) on a Perkin-Elmer 377 spectrophotometer in KBr with absorption in cm^{-1}. ^{1}H-NMR and ^{13}C-NMR spectra were recorded on Bruker AV 400 and 100 MHz using DMSO-d6 as solvent and TMS as an internal standard. Chemical shifts are reported in parts per million (δ in ppm) relative to the designated referenced peaks: DMSO-d_6 at 2.5, 3.33 ppm. When peak multiplicities are reported, the following abbreviations are used: s = singlet, d = doublet, t = triplet q = quartet, m = multiplet, br = broadened, dd = doublet of doublets. Coupling constants (*J*) were reported in (Hertz) Hz. ^{1}H NMR and ^{13}C NMR were recorded at 300 K temperature and other details as mentioned in NMR spectra. Mass spectra were recorded on Advion Expression CMS, USA, using ACN: Water: Formic acid (70: 30: 0.1%) as mobile phase. Important parameter of Mass spectra: DL temperature: 300℃, heat block: 300℃, drying gas flow: 20 Litter/Minute, run time: 1 minute, flow: 0.5mL/Min., range mass: 0-1500 m/z, oven temperature: 40℃, nebulizing gas flow: 4.4 Litter/minute, cooler temperature: 25℃ and detector: UV. ESI Mass analysis parameter: capillary temperature: 250℃, source temperature: 300℃, capillary voltage: 1.5 volts, MeOH: Water: Formic acid (90: 10: 0.1%) as mobile phase. Elemental analysis was performed as per standard protocol on vario MICRO cube, elementar CHNS analyzer serial no.: 15084053. Molecular docking and Molecular dynamics were done using the YASARA commercial package. Pose visualization of molecular docking and molecular dynamics was carried out using Schrodinger Maestro 11, LLC, New York, 2015. ADMET properties of novel compounds were foretold using the Accelrys Discovery Studio 2.1 software. DruliTo software was used to get drug-likeness properties (Lipinski's Rule of Five).

2.2. General procedure for the synthesis of compound (5a-5ao):

In 25 ml round-bottomed flask, a mixture of 2-(3-(4-substituted phenyl)-4,5-dihydro-1H-pyrazol-5-yl)phenol derivatives **4a**-**4o** (1 eq.) and isatin derivatives (1 eq.) with 5 ml DMF were subjected to microwave (CEM microwave) at 450W (150 °C) for 6-12 minutes in the presence of *p*-TSA (1 eq.). The progress of the reaction was monitored by TLC (30% ethyl acetate-hexane). The reaction mixture was allowed to cool at room temperature. The reaction mixture was then poured into ice water and the resulting solid residues were filtered off, dried to get the crude product which was further recrystallized from methanol or ethanol to yield 2-(4-substituted

phenyl)-1,10b dihydrospiro [benzo[e]pyrazolo[1,5-c][1,3]oxazine-5,3'-indolin]-2'-one **(*5a-5ao*)** in very good yields with good purity.[25]

2.3. General procedure for the synthesis of compound (6a-6ao):

To a stirred solution of 2-(substituted phenyl)-1,10bdihydrospiro[benzo[e]pyrazolo[1,5-c][1,3] oxazine-5,3'-indolin]-2'-one (**5a-5ao**) (1 eq.) in acetonitrile (10V) was added triethylamine (2 eq.) at room temperature. To this, chloroacetyl chloride (1.2 eq.) was added dropwise at 0 °C to the reaction mixture. The resulting solution was stirred at room temperature for 3h. The reaction mixture was then poured into water, and extracted with DCM. The combined organic layer was washed with 1M aq. solution of NaOH, & brine solution and dried over Na_2SO_4, filtered and evaporated to afford chloroacetyl adduct of (**5a-5ao**). Furthermore, Isoniazid (1 eq) and triethylamine (0.26 mmol, 1.5 equiv.) were refluxed with above obtained chloroacetyl adduct of (**5a-5ao,** 1 eq.) for 4h. The progress of the reaction was monitored by TLC. After completion of the reaction, the reaction mixture was transferred onto ice/cold water and the separated solid was then filtered, washed with water, and dried well in a rotary evaporator. The crude product was further purified by gravitational column chromatography using 15-30% Ethyl acetate: hexane as eluent. Pure fractions were evaporated to dryness. The column purified compound further triturated using 10-20% diethyl ether in n-pentane to afford highly pure (>95%) title compound **(6a-6ao)** with good practical yield.

Characterizations Data:

2.3.1. N'-(2-oxo-2-(2'-oxo-2-phenyl-1,10b-dihydrospiro[benzo[e]pyrazolo[1,5-c][1,3]oxazine-5,3'-indolin]-1'-yl)ethyl)isonicotinohydrazide (6a):

Brown solid; IR (KBr) (υmax, cm^{-1}): 3255 (C-H Aromatic), 1616 ($C=N_{str}$), 1724 ($C=O_{str}$), 1213 (C-O ether); ^{1}H NMR (400 MHz, DMSO) δ 11.86 (s, 1H), 8.95 (d, *J* = 7.5 Hz, 2H), 7.95 (d, *J* = 7.2 Hz, 2H), 7.79 (dd, *J* = 7.4, 1.4 Hz, 1H), 7.56 (dd, *J* = 7.6, 1.5 Hz, 1H), 7.54 - 7.46 (m, 2H), 7.44 (dd, *J* = 7.6, 1.5 Hz, 1H), 7.35 (dd, *J* = 7.4, 1.4 Hz, 1H), 7.27 (dtdd, *J* = 12.9, 7.2, 5.9, 1.6 Hz, 5H), 7.10 (td, *J* = 7.6, 1.5 Hz, 1H), 6.98 (dd, *J* = 7.4, 1.4 Hz, 1H), 5.49 (t, *J* = 6.4 Hz, 1H), 4.17 (s, 1H), 3.90 (s, 1H), 3.74 (s, 1H), 2.67 (dd, *J* = 12.4, 6.4 Hz, 1H), 2.42 (dd, *J* = 12.4, 6.4 Hz, 1H); ^{13}C NMR (100 MHz, DMSO) δ 175.32, 167.84, 164.23, 154.15, 150.99, 145.86, 143.94, 139.99, 134.71, 132.76, 130.29, 129.32, 128.59, 127.52, 127.25, 125.81, 123.85, 123.03, 120.06, 119.58, 116.20, 111.55, 60.70, 53.75, 38.96; ESI-MS: m/z Calculated 544.57, found $[M+H]^+$ 545.5; Anal. Calcd for $C_{31}H_{24}N_6O_4$: C, 68.37; H, 4.44; N, 15.43; O, 11.75%; found C, 68.45; H, 4.82; N, 15.20%.

2.3.2. N'-(2-(2-(4-chlorophenyl)-2'-oxo-1,10b-dihydrospiro[benzo[e]pyrazolo[1,5-c][1,3]oxazine-5,3'-indolin]-1'-yl)-2-oxoethyl)isonicotinohydrazide **(6b):**

Saddle Brown solid; IR (KBr) (υmax, cm^{-1}): 3150 (C-H Aromatic), 1688 ($C=N_{str}$), 1720 ($C=O_{str}$), 1212 (C-O ether); ^{1}H NMR (400 MHz, DMSO) δ 8.95 (d, *J* = 7.5 Hz, 2H), 8.52 (s, 1H), 7.91 (d, *J* = 7.5 Hz, 2H), 7.78 (dd, *J* = 7.6, 1.5 Hz, 1H), 7.48 (tdd, *J* = 15.2, 7.6, 1.5 Hz, 4H), 7.32 (dd, *J* = 7.4, 2.5 Hz, 3H), 7.24 (ddd, *J* = 16.3, 7.6, 1.4 Hz, 2H), 7.07 (td, *J* = 7.6, 1.5 Hz, 1H), 6.97 (dd, *J* = 7.6, 1.5 Hz, 1H), 5.29 (t, *J* = 6.1 Hz, 1H), 4.15 (s, 1H), 4.11 (s, 1H), 3.90 (s, 1H), 2.67 (dd, *J* = 12.4, 6.0 Hz, 1H), 2.42 (dd, *J* = 12.5, 6.1 Hz, 1H); ^{13}C NMR (100 MHz, DMSO) δ 175.32,

167.84, 164.23, 154.15, 150.99, 145.86, 143.94, 139.99, 134.78, 132.53, 130.29, 129.32, 129.05, 127.77, 127.52, 127.25, 123.85, 123.03, 120.06, 119.58, 116.20, 111.55, 60.70, 53.75, 38.96; ESI-MS: m/z Calculated 579.01, found $[M+H]^+$ 580.0; Anal. Calcd for $C_{31}H_{23}ClN_6O_4$: C, 64.31; H, 4.00; Cl, 6.12; N, 14.51; O, 11.05%; found C, 64.69; H, 4.30; N, 14.35%.

***2.3.3. N'-(2-(2-(4-bromophenyl)-2'-oxo-1,10b-dihydrospiro[benzo[e]pyrazolo[1,5-c][1,3]oxazine-5,3'-indolin]-1'-yl)-2-oxoethyl)isonicotinohydrazide* (6c):**

Burly Wood solid; IR (KBr) (υmax, cm^{-1}): 3200 (C-H Aromatic), 1675 ($C=N_{str}$), 1812 ($C=O_{str}$), 1200 (C-O ether); ^{1}H NMR (400 MHz, DMSO) δ 8.95 (d, *J* = 7.5 Hz, 2H), 8.58 (s, 1H), 7.90 (d, *J* = 7.5 Hz, 2H), 7.79 (dd, *J* = 7.4, 1.4 Hz, 1H), 7.62 - 7.53 (m, 1H), 7.50 (d, *J* = 26.5 Hz, 1H), 7.47 - 7.32 (m, 4H), 7.26 (dddd, *J* = 15.1, 11.2, 7.6, 1.5 Hz, 3H), 7.07 (td, *J* = 7.5, 1.4 Hz, 1H), 6.97 (dd, *J* = 7.4, 1.4 Hz, 1H), 5.09 (t, *J* = 5.8 Hz, 1H), 4.13 (s, 1H), 4.02 (s, 1H), 3.96 (s, 1H), 2.67 (dd, *J* = 12.4, 6.0 Hz, 1H), 2.42 (dd, *J* = 12.5, 5.8 Hz, 1H); ^{13}C NMR (100 MHz, DMSO) δ 175.32, 167.84, 164.23, 154.15, 150.99, 145.86, 143.94, 139.99, 134.71, 131.98, 131.57, 130.29, 129.32, 127.52, 127.25, 126.33, 123.85, 123.03, 121.78, 120.06, 119.58, 116.20, 111.55, 60.70, 53.75, 38.96; ESI-MS: m/z Calculated 623.47, found $[M+H]^+$ 624.4; Anal. Calcd for $C_{31}H_{23}BrN_6O_4$: C, 59.72; H, 3.72; Br, 12.82; N, 13.48; O, 10.26%; found C, 59.89; H, 3.58; N, 13.27%.

***2.3.4. N'-(2-(2-(4-aminophenyl)-2'-oxo-1,10b-dihydrospiro[benzo[e]pyrazolo[1,5-c][1,3]oxazine-5,3'-indolin]-1'-yl)-2-oxoethyl)isonicotinohydrazide* (6d):**

Saddle Brown solid; IR (KBr) (υmax, cm^{-1}): 3100 (C-H Aromatic), 1610 ($C=N_{str}$), 1700 ($C=O_{str}$), 1100 (C-O ether); ^{1}H NMR (400 MHz, DMSO) δ 13.40 (s, 1H), 8.95 (d, *J* = 7.5 Hz, 2H), 7.97 (d, *J* = 7.5 Hz, 2H), 7.87 - 7.72 (m, 1H), 7.63 – 7.48 (m, 1H), 7.45 (td, *J* = 7.6, 1.5 Hz, 1H), 7.40 - 7.33 (m, 3H), 7.25 (ddd, *J* = 15.6, 7.7, 1.5 Hz, 2H), 7.10 (td, *J* = 7.5, 1.4 Hz, 1H), 7.04 – 6.90 (m, 1H), 6.67 (d, *J* = 7.5 Hz, 2H), 5.72 (t, *J* = 7.1 Hz, 1H), 5.29 (s, 2H), 4.13 (s, 1H), 3.93 (s, 1H), 3.72 (s, 1H), 3.67 (dd, *J* = 12.4, 7.1 Hz, 1H), 2.42 (dd, *J* = 12.4, 7.1 Hz, 1H); ^{13}C NMR (100 MHz, DMSO) δ 175.32, 167.84, 164.23, 154.15, 150.99, 147.40, 145.86, 143.94, 139.99, 134.71, 130.29, 129.32, 127.52, 127.25, 126.93, 123.85, 123.03, 122.22, 120.06, 119.58, 116.20, 113.58, 111.55, 60.70, 53.75, 38.96; ESI-MS: m/z Calculated 599.59, found $[M+H]^+$ 600.5; Anal. Calcd for $C_{31}H_{25}N_7O_4$: C, 66.54; H, 4.50; N, 17.52; O, 11.44%; found C, 66.28; H, 4.43; N, 17.37%.

***2.3.5. N'-(2-(2-(4-hydroxyphenyl)-2'-oxo-1,10b-dihydrospiro[benzo[e]pyrazolo[1,5-c][1,3]oxazine-5,3'-indolin]-1'-yl)-2-oxoethyl)isonicotinohydrazide* (6e):**

Gray solid; IR (KBr) (υmax, cm^{-1}): 3132 (C-H Aromatic), 1593 (C=Nstr), 1702 (C=Ostr), 1300 (C-O ether) ; ^{1}H NMR (400 MHz, DMSO) δ 11.42 (s, 1H), 8.95 (d, *J* = 7.5 Hz, 2H), 8.37 (s, 1H), 7.94 (d, *J* = 7.5 Hz, 2H), 7.77 (dd, *J* = 7.4, 1.4 Hz, 1H), 7.62 – 7.46 (m, 1H), 7.44 (dt, *J* = 7.3, 3.6 Hz, 1H), 7.40 - 7.29 (m, 3H), 7.25 (dd, *J* = 10.8, 4.3 Hz, 2H), 7.10 (td, *J* = 7.4, 1.4 Hz, 1H), 6.98 (dd, *J* = 7.4, 1.4 Hz, 1H), 6.79 (d, *J* = 7.5 Hz, 2H), 5.69 (t, *J* = 6.2 Hz, 1H), 4.42 (s, 1H), 3.74 (s, 1H), 3.44 (s, 1H), 2.67 (dd, *J* = 12.6, 6.2 Hz, 1H), 2.42 (dd, *J* = 12.4, 6.2 Hz, 1H); ^{13}C NMR (100 MHz, DMSO) δ 175.32, 167.84, 164.23, 159.08, 154.15, 150.99, 145.86, 143.94, 139.99, 134.71, 130.29, 129.32, 128.09, 127.52, 127.25, 124.84, 123.85, 123.03, 120.06, 119.58, 116.20, 115.78,

111.55, 60.70, 53.75, 38.96; ESI-MS: m/z Calculated 560.57, found $[M+H]^+$ 561.5; Anal. Calcd for $C_{31}H_{24}N_6O_5$: C, 66.42; H, 4.32; N, 14.99; O, 14.27%; found C, 66.82; H, 4.63; N, 14.40%.

***2.3.6. N'-(2-oxo-2-(2'-oxo-2-(p-tolyl)-1,10b-dihydrospiro[benzo[e]pyrazolo[1,5-c][1,3]oxazine-5,3'-indolin]-1'-yl)ethyl)isonicotinohydrazide* (6f):**

Brown solid; IR (KBr) (υmax, cm^{-1}): 3245 (C-H Aromatic), 1623 ($C=N_{str}$), 1810 ($C=O_{str}$), 1298 (C-O ether); ^1H NMR (400 MHz, DMSO) δ 8.95 (d, *J* = 7.5 Hz, 2H), 8.53 (s, 1H), 7.91 (d, *J* = 7.5 Hz, 2H), 7.78 (dd, *J* = 7.4, 1.4 Hz, 1H), 7.57 - 7.47 (m, 3H), 7.44 (td, *J* = 7.4, 1.4 Hz, 1H), 7.32 (dd, *J* = 7.4, 1.4 Hz, 1H), 7.24 (ddd, *J* = 16.3, 7.6, 1.5 Hz, 2H), 7.17 (d, *J* = 7.5 Hz, 2H), 7.08 (td, *J* = 7.4, 1.4 Hz, 1H), 6.97 (dd, *J* = 7.4, 1.4 Hz, 1H), 5.30 (t, *J* = 6.2 Hz, 1H), 4.16 (s, 1H), 4.11 (s, 1H), 3.90 (s, 1H), 2.67 (dd, *J* = 12.4, 6.0 Hz, 1H), 2.42 (dd, *J* = 12.5, 6.1 Hz, 1H), 2.29 (s, 3H); ^{13}C NMR (100 MHz, DMSO) δ 175.32, 167.84, 164.23, 154.15, 150.99, 145.86, 143.94, 139.99, 139.17, 134.71, 131.77, 130.29, 129.32, 128.97, 127.52, 127.25, 125.43, 123.85, 123.03, 120.06, 119.58, 116.20, 111.55, 60.70, 53.75, 38.96, 21.12; ESI-MS: m/z Calculated 558.60, found $[M+H]^+$ 559.6; Anal. Calcd for $C_{32}H_{26}N_6O_4$: C, 68.81; H, 4.69; N, 15.05; O, 11.46%; found C, 68.42; H, 4.34; N, 15.25%.

***2.3.7. N'-(2-(2-(4-fluorophenyl)-2'-oxo-1,10b-dihydrospiro [benzo[e] pyrazolo [1,5-c][1,3] oxazine-5,3'-indolin]-1'-yl)-2-oxoethyl)isonicotinohydrazide* (6g):**

Sienna Brown solid; IR (KBr) (υmax, cm^{-1}): 3214 (C-H Aromatic), 1685 (C=Nstr), 1728 (C=Ostr), 1110 (C-O ether); ^1H NMR (400 MHz, DMSO) δ 8.95 (d, *J* = 7.5 Hz, 2H), 8.79 (s, 1H), 7.90 (d, *J* = 7.5 Hz, 2H), 7.76 (dd, *J* = 7.6, 1.3 Hz, 1H), 7.54 (dd, *J* = 7.6, 1.5 Hz, 1H), 7.51 - 7.47 (m, 2H), 7.44 (td, *J* = 7.6, 1.4 Hz, 1H), 7.31 (dd, *J* = 7.4, 1.4 Hz, 1H), 7.25 (tdd, *J* = 7.5, 4.6, 1.4 Hz, 2H), 7.08 (td, *J* = 7.4, 1.4 Hz, 1H), 7.04 (t, *J* = 7.8 Hz, 2H), 6.97 (dd, *J* = 7.4, 1.4 Hz, 1H), 5.12 (t, *J* = 5.7 Hz, 1H), 4.34 (s, 1H), 4.09 (s, 1H), 4.02 (s, 1H), 2.67 (dd, *J* = 12.6, 5.7 Hz, 1H), 2.42 (dd, *J* = 12.4, 5.7 Hz, 1H); ^{13}C NMR (100 MHz, DMSO) δ 175.32, 167.84, 164.23, 163.10, 160.48, 154.15, 150.99, 145.86, 143.94, 139.99, 134.71, 130.29, 129.29, 128.32, 127.52, 127.25, 123.85, 123.03, 120.06, 119.58, 116.37, 111.55, 60.70, 53.75, 38.96; ESI-MS: m/z Calculated 562.56, found $[M+H]^+$ 563.5; Anal. Calcd for $C_{31}H_{23}FN_6O_4$: C, 66.19; H, 4.12; F, 3.38; N, 14.94; O, 11.38%; found C, 66.30; H, 4.41; N, 14.85%.

***2.3.8. N'-(2-(2-(3-bromophenyl)-2'-oxo-1,10b-dihydrospiro [benzo[e]pyrazolo [1,5-c][1,3] oxazi ne-5,3'-indolin]-1'-yl)-2-oxoethyl)isonicotinohydrazide* (6h):**

Brown solid; IR (KBr) (υmax, cm^{-1}): 3135 (C-H Aromatic), 1600 ($C=N_{str}$), 1721 ($C=O_{str}$), 1285 (C-O ether); ^1H NMR (400 MHz, DMSO) δ 8.95 (d, *J* = 7.5 Hz, 2H), 8.53 (s, 1H), 7.91 (d, *J* = 7.5 Hz, 2H), 7.84 - 7.76 (m, 2H), 7.61 - 7.44 (m, 3H), 7.43 (dd, *J* = 2.9, 1.5 Hz, 1H), 7.32 (dd, *J* = 7.4, 1.4 Hz, 1H), 7.24 (ddd, *J* = 14.5, 7.4, 1.4 Hz, 2H), 7.19 (t, *J* = 7.6 Hz, 1H), 7.08 (td, *J* = 7.6, 1.5 Hz, 1H), 6.97 (dd, *J* = 7.4, 1.4 Hz, 1H), 5.29 (t, *J* = 6.1 Hz, 1H), 4.15 (s, 1H), 4.11 (s, 1H), 3.90 (s, 1H), 2.67 (dd, *J* = 12.4, 6.0 Hz, 1H), 2.42 (dd, *J* = 12.4, 6.0 Hz, 1H); ^{13}C NMR (100 MHz, DMSO) δ 175.32, 167.84, 164.23, 154.15, 150.99, 145.08, 143.94, 139.99, 134.69, 130.29, 130.05, 129.80, 129.32, 127.61, 127.25, 124.63, 123.85, 123.03, 120.06, 119.58, 116.20, 111.55, 60.70, 53.75, 38.96; ESI-MS: m/z Calculated 623.47, found $[M+H]^+$ 624.4; Anal. Calcd for

$C_{31}H_{23}BrN_6O_4$: C, 59.72; H, 3.72; Br, 12.82; N, 13.48; O, 10.26%; found C, 59.39; H, 3.38; N, 13.27%.

***2.3.9. N'-(2-(2-(4-nitrophenyl)-2'-oxo-1,10b-dihydrospiro[benzo[e]pyrazolo[1,5-c][1,3] oxazine-5,3'-indolin]-1'-yl)-2-oxoethyl)isonicotinohydrazide* (6i):**

Burly Wood solid; IR (KBr) (υmax, cm^{-1}): 3155 (C-H Aromatic), 1612 ($C=N_{str}$), 1642 ($C=O_{str}$), 1202 (C-O ether); ^{1}H NMR (400 MHz, DMSO) δ 8.95 (d, *J* = 7.2 Hz, 2H), 8.75 (s, 1H), 8.23 (d, *J* = 7.5 Hz, 2H), 7.90 (d, *J* = 7.4 Hz, 2H), 7.76 (d, *J* = 7.5 Hz, 2H), 7.52 - 7.34 (m, 3H), 7.28 - 7.22 (m, 2H), 7.09 (td, *J* = 7.5, 1.5 Hz, 1H), 6.97 (dd, *J* = 7.4, 1.5 Hz, 1H), 5.45 (t, *J* = 6.0 Hz, 1H), 4.38 (s, 1H), 4.32 (s, 1H), 3.57 (s, 1H), 2.67 (dd, *J* = 12.4, 6.0 Hz, 1H), 2.42 (dd, *J* = 12.5, 6.0 Hz, 1H); ^{13}C NMR (100 MHz, DMSO) δ 175.32, 167.84, 164.23, 154.15, 150.99, 146.30, 145.86, 143.94, 139.99, 136.93, 134.71, 130.29, 129.32, 127.52, 127.25, 125.51, 123.85, 123.03, 120.06, 119.58, 116.20, 111.55, 60.70, 53.75, 38.96; ESI-MS: m/z Calculated 589.57, found $[M+H]^+$ 590.5; Anal. Calcd for $C_{31}H_{23}N_7O_6$: C, 63.15; H, 3.93; N, 16.63; O, 16.28%; found C, 63.58; H, 3.63; N, 16.95%.

***2.3.10. N'-(2-(2-(2-hydroxyphenyl)-2'-oxo-1,10b-dihydrospiro[benzo[e]pyrazolo[1,5-c][1,3] oxazine-5,3'-indolin]-1'-yl)-2-oxoethyl)isonicotinohydrazide* (6j):**

Greenish Brown solid; IR (KBr) (υmax, cm^{-1}): 3125 (C-H Aromatic), 1618 ($C=N_{str}$), 1678 ($C=O_{str}$), 1268 (C-O ether); ^{1}H NMR (400 MHz, DMSO) δ 10.00 (s, 1H), 8.96 (d, *J* = 7.4 Hz, 2H), 8.64 (s, 1H), 7.90 (d, *J* = 7.4 Hz, 2H), 7.52 – 7.44 (m, 2H), 7.44 - 7.29 (m, 3H), 7.24 (dtd, *J* = 17.5, 7.4, 1.6 Hz, 2H), 7.10 (dtd, *J* = 10.3, 7.5, 1.5 Hz, 2H), 7.01 (dd, *J* = 7.5, 1.4 Hz, 1H), 6.87 (td, *J* = 7.5, 1.4 Hz, 1H), 6.78 (dd, *J* = 7.5, 1.4 Hz, 1H), 5.52 (t, *J* = 9.0 Hz, 1H), 4.91 (s, 1H), 3.93 (s, 1H), 3.69 (s, 1H), 2.74 - 2.65 (m, 1H), 2.44 - 2.36 (m, 1H); ^{13}C NMR (100 MHz, DMSO) δ 175.32, 167.84, 164.23, 157.79, 154.15, 150.99, 143.94, 139.99, 138.27, 134.71, 130.29, 129.84, 129.32, 127.81, 127.52, 127.25, 123.85, 123.03, 121.25, 120.06, 119.58, 118.65, 116.20, 115.54, 111.55, 60.70, 53.75, 38.89; ESI-MS: m/z Calculated 560.57, found $[M+H]^+$ 561.5; Anal. Calcd for $C_{31}H_{24}N_6O_5$: C, 66.42; H, 4.32; N, 14.99; O, 14.27%; found C, 66.65; H, 4.61; N, 14.49%.

***2.3.11. N'-(2-(2-(4-methoxyphenyl)-2'-oxo-1,10b-dihydrospiro[benzo[e]pyrazolo[1,5-c][1,3] oxazine-5,3'-indolin]-1'-yl)-2-oxoethyl)isonicotinohydrazide* (6k):**

Saddle Brown solid; IR (KBr) (υmax, cm^{-1}): 3254 (C-H Aromatic), 1612 ($C=N_{str}$), 1671 ($C=O_{str}$), 1145 (C-O ether); ^{1}H NMR (400 MHz, DMSO) δ 8.95 (d, *J* = 7.4 Hz, 2H), 8.53 (s, 1H), 7.90 (d, *J* = 7.4 Hz, 2H), 7.78 (dd, *J* = 7.4, 1.5 Hz, 1H), 7.48 (tdd, *J* = 15.0, 7.5, 1.5 Hz, 4H), 7.42 – 7.20 (m, 3H), 7.10 (td, *J* = 7.4, 1.5 Hz, 1H), 7.02 - 6.82 (m, 3H), 5.34 (t, *J* = 6.8 Hz, 1H), 4.63 (s, 1H), 4.18 (s, 1H), 3.78 (s, 4H), 2.67 (dd, *J* = 12.4, 6.7 Hz, 1H), 2.42 (dd, *J* = 12.5, 6.8 Hz, 1H); ^{13}C NMR (100 MHz, DMSO) δ 175.32, 167.84, 164.23, 159.72, 154.15, 150.99, 145.86, 143.94, 139.99, 134.71, 130.29, 129.32, 127.36, 126.78, 123.85, 123.03, 120.06, 119.58, 116.20, 114.84, 111.55, 60.70, 56.03, 53.75, 38.96; ESI-MS: m/z Calculated 574.60, found $[M+H]^+$ 575.6; Anal. Calcd for $C_{32}H_{26}N_6O_5$: C, 66.89; H, 4.56; N, 14.63; O, 13.92%; found C, 66.47; H, 4.93; N, 14.47%.

2.3.12. N'-(2-(2-(2-chlorophenyl)-2'-oxo-1,10b-dihydrospiro[benzo[e]pyrazolo[1,5-c][1,3]

***oxazine-5,3'-indolin]-1'-yl)-2-oxoethyl)isonicotinohydrazide* (6l):**

Gray solid; IR (KBr) (υmax, cm^{-1}): 3165 (C-H Aromatic), 1617 ($C=N_{str}$), 1759 ($C=O_{str}$), 1123 (C-O ether); ^1H NMR (400 MHz, DMSO) δ 8.92 (d, *J* = 7.4 Hz, 2H), 7.90 - 7.81 (m, 3H), 7.81 - 7.63 (m, 1H), 7.62 – 7.48 (m, 2H), 7.45 (td, *J* = 7.5, 1.4 Hz, 1H), 7.39 - 7.16 (m, 6H), 7.12 (td, *J* = 7.4, 1.5 Hz, 1H), 7.00 (dd, *J* = 7.5, 1.4 Hz, 1H), 5.31 (t, *J* = 7.7 Hz, 1H), 4.20 (s, 1H), 3.93 (s, 1H), 3.63 (s, 1H), 2.69 - 2.65 (m, 1H), 2.44 - 2.40 (m, 1H); ^{13}C NMR (100 MHz, DMSO) δ 175.32, 167.84, 164.23, 154.15, 150.99, 144.48, 143.94, 139.99, 134.71, 133.42, 131.78, 130.20, 129.32, 127.82, 127.52, 127.25, 126.84, 123.85, 123.03, 120.06, 119.58, 116.20, 111.55, 60.70, 53.75, 38.89; ESI-MS: m/z Calculated 579.01, found $[M+H]^+$ 580.0; Anal. Calcd for $C_{31}H_{23}ClN_6O_4$: C, 64.31; H, 4.00; Cl, 6.12; N, 14.51; O, 11.05%; found C, 64.67; H, 4.30; N, 14.38%.

***2.3.13. N'-(2-(2-(3-nitrophenyl)-2'-oxo-1,10b-dihydrospiro[benzo[e]pyrazolo[1,5-c][1,3] oxazine-5,3'-indolin]-1'-yl)-2-oxoethyl)isonicotinohydrazide* (6m):**

Brown solid; IR (KBr) (υmax, cm^{-1}): 3102 (C-H Aromatic), 1660 ($C=N_{str}$), 1704 ($C=O_{str}$), 1071 (C-O ether); ^1H NMR (400 MHz, DMSO) δ 8.90 (d, *J* = 7.4 Hz, 2H), 8.62 (s, 1H), 8.53 (t, *J* = 1.4 Hz, 1H), 8.19 (dt, *J* = 7.5, 1.4 Hz, 1H), 7.98 - 7.82 (m, 3H), 7.80 (dd, *J* = 7.5, 1.5 Hz, 1H), 7.55 (t, *J* = 7.5 Hz, 1H), 7.49 (dd, *J* = 7.5, 1.5 Hz, 1H), 7.47 - 7.39 (m, 2H), 7.24 (dtd, *J* = 9.0, 7.4, 1.4 Hz, 2H), 7.10 (td, *J* = 7.5, 1.5 Hz, 1H), 6.80 (dd, *J* = 7.5, 1.4 Hz, 1H), 5.17 (t, *J* = 6.4 Hz, 1H), 4.49 (s, 1H), 3.66 (s, 1H), 2.98 (s, 1H), 2.67 (dd, *J* = 12.5, 6.4 Hz, 1H), 2.42 (dd, *J* = 12.5, 6.4 Hz, 1H); ^{13}C NMR (100 MHz, DMSO) δ 175.32, 167.84, 164.23, 154.15, 150.99, 147.74, 145.08, 143.94, 139.99, 135.81, 134.71, 130.36, 129.30, 127.52, 127.25, 124.10, 123.85, 123.03, 121.84, 120.06, 119.58, 116.20, 111.55, 60.70, 53.75, 38.96; ESI-MS: m/z Calculated 589.57, found $[M+H]^+$ 590.5; Anal. Calcd for $C_{31}H_{23}N_7O_6$: C, 63.15; H, 3.93; N, 16.63; O, 16.28%; found C, 63.37; H, 3.44; N, 16.41%.

***2.3.14. N'-(2-(2-(2,4-dichlorophenyl)-2'-oxo-1,10b-dihydrospiro[benzo[e]pyrazolo[1,5-c][1,3] oxazine-5,3'-indolin]-1'-yl)-2-oxoethyl)isonicotinohydrazide* (6n):**

Brown solid; IR (KBr) (υmax, cm^{-1}): 3269 (C-H Aromatic), 1640 ($C=N_{str}$), 1724 ($C=O_{str}$), 1081 (C-O ether); ^1H NMR (400 MHz, DMSO) δ 8.92 (d, *J* = 7.4 Hz, 2H), 7.94 - 7.78 (m, 3H), 7.69 (dd, *J* = 7.5, 1.4 Hz, 1H), 7.54 (dd, *J* = 7.5, 1.4 Hz, 1H), 7.45 - 7.31 (m, 4H), 7.31 - 7.08 (m, 4H), 7.01 (dd, *J* = 7.4, 1.5 Hz, 1H), 5.08 (t, *J* = 6.9 Hz, 1H), 4.22 (s, 1H), 3.71 (s, 1H), 3.32 (s, 1H), 2.67 (dd, *J* = 12.4, 6.9 Hz, 1H), 2.42 (dd, *J* = 12.4, 6.9 Hz, 1H); ^{13}C NMR (100 MHz, DMSO) δ 175.32, 167.84, 164.23, 154.15, 150.99, 144.48, 143.94, 139.99, 134.71, 133.42, 132.99, 132.69, 130.55, 130.29, 129.32, 128.41, 127.86, 127.52, 127.25, 123.85, 123.03, 120.06, 119.58, 116.20, 111.55, 60.70, 53.75, 38.89; ESI-MS: m/z Calculated 613.46, found $[M+H]^+$ 614.4; Anal. Calcd for $C_{31}H_{22}Cl_2N_6O_4$: C, 60.70; H, 3.61; Cl, 11.56; N, 13.70; O, 10.43%; found C, 60.45; H, 3.24; N, 13.55%.

***2.3.15. N'-(2-(2-(2-methoxyphenyl)-2'-oxo-1,10b-dihydrospiro[benzo[e]pyrazolo[1,5-c][1,3] oxazine-5,3'-indolin]-1'-yl)-2-oxoethyl)isonicotinohydrazide* (6o):**

Saddle Brown solid; IR (KBr) (υmax, cm^{-1}): 3240 (C-H Aromatic), 1681 ($C=N_{str}$), 1729 ($C=O_{str}$), 1207 (C-O ether); ^1H NMR (400 MHz, DMSO) δ 8.95 (d, *J* = 7.4 Hz, 2H), 8.61 (s, 1H), 7.91 (d,

J = 7.4 Hz, 2H), 7.79 (dd, *J* = 7.4, 1.5 Hz, 1H), 7.66 - 7.42 (m, 3H), 7.40 - 7.19 (m, 4H), 7.06 (ddd, *J* = 14.5, 7.4, 1.4 Hz, 2H), 6.98 (ddd, *J* = 11.4, 7.5, 1.5 Hz, 2H), 5.13 (t, *J* = 5.3 Hz, 1H), 4.33 (s, 1H), 4.14 (s, 1H), 3.87 (s, 1H), 3.76 (s, 3H), 2.67 (dd, *J* = 12.5, 5.3 Hz, 1H), 2.42 (dd, *J* = 12.5, 5.3 Hz, 1H); ^{13}C NMR (100 MHz, DMSO) δ 175.32, 167.84, 164.23, 158.35, 154.15, 150.99, 143.94, 139.99, 136.73, 134.71, 130.29, 129.32, 128.31, 127.52, 127.26, 123.77, 123.03, 121.85, 120.06, 119.58, 116.20, 114.88, 111.55, 60.70, 56.78, 53.75, 38.89; ESI-MS: m/z Calculated 574.60, found $[M+H]^+$ 575.6; Anal. Calcd for $C_{32}H_{26}N_6O_5$: C, 66.89; H, 4.56; N, 14.63; O, 13.92%; found C, 66.37; H, 4.38; N, 14.22%.

***2.3.16. N'-(2-(5'-chloro-2'-oxo-2-phenyl-1,10b-dihydrospiro[benzo[e]pyrazolo[1,5-c][1,3] oxazine-5,3'-indolin]-1'-yl)-2-oxoethyl)isonicotinohydrazide* (6aa):**

Gray solid; IR (KBr) (υmax, cm^{-1}): 3155 (C-H Aromatic), 1630 ($C=N_{str}$), 1738 ($C=O_{str}$), 1227 (C-O ether); ^{1}H NMR (400 MHz, DMSO) δ 12.67 (s, 1H), 8.90 (d, *J* = 7.4 Hz, 2H), 7.85 (d, *J* = 7.2 Hz, 2H), 7.74 (d, *J* = 7.5 Hz, 1H), 7.64 (d, *J* = 1.4 Hz, 1H), 7.57 - 7.45 (m, 2H), 7.45 - 7.35 (m, 1H), 7.35 - 7.23 (m, 5H), 7.10 (td, *J* = 7.5, 1.5 Hz, 1H), 6.89 (dd, *J* = 7.4, 1.5 Hz, 1H), 5.07 (t, *J* = 5.8 Hz, 1H), 4.24 (s, 1H), 3.59 (s, 1H), 3.46 (s, 1H), 2.67 (dd, *J* = 12.4, 5.8 Hz, 1H), 2.42 (dd, *J* = 12.4, 5.8 Hz, 1H); ^{13}C NMR (100 MHz, DMSO) δ 175.32, 167.84, 164.23, 154.15, 150.99, 145.86, 143.98, 139.99, 136.05, 134.33, 132.76, 130.29, 128.59, 127.52, 126.17, 125.81, 123.85, 123.12, 120.06, 116.20, 113.30, 60.70, 53.75, 38.9;. ESI-MS: m/z Calculated 579.01, found $[M+H]^+$ 580.0; Anal. Calcd for $C_{31}H_{23}ClN_6O_4$: C, 64.31; H, 4.00; Cl, 6.12; N, 14.51; O, 11.05%; found C, 64.68; H, 4.33; N, 14.96%.

***2.3.17. N'-(2-(5'-chloro-2-(4-chlorophenyl)-2'-oxo-1,10b-dihydrospiro[benzo[e] pyrazolo[1,5-c][1,3]oxazine-5,3'-indolin]-1'-yl)-2-oxoethyl)isonicotinohydrazide* (6ab):**

Saddle Brown solid; IR (KBr) (υmax, cm^{-1}): 3270 (C-H Aromatic), 1614 ($C=N_{str}$), 1769 ($C=O_{str}$), 1200 (C-O ether); ^{1}H NMR (400 MHz, DMSO) δ 9.66 (s, 1H), 8.96 (d, *J* = 7.4 Hz, 2H), 7.75 (dd, *J* = 8.9, 4.4 Hz, 3H), 7.48 (dd, *J* = 7.5, 1.4 Hz, 1H), 7.45 - 7.29 (m, 5H), 7.29 - 7.22 (m, 2H), 7.07 (td, *J* = 7.6, 1.5 Hz, 1H), 7.01 (dd, *J* = 7.3, 1.4 Hz, 1H), 4.63 (t, *J* = 5.8 Hz, 1H), 3.86 (s, 1H), 3.80 (s, 1H), 3.74 (s, 1H), 2.89 (dd, *J* = 12.4, 5.8 Hz, 1H), 2.42 (dd, *J* = 12.4, 5.8 Hz, 1H); ^{13}C NMR (100 MHz, DMSO) δ 175.32, 167.84, 164.23, 154.15, 150.99, 145.86, 143.98, 139.99, 136.05, 134.85, 134.33, 132.53, 130.29, 129.05, 127.77, 127.52, 126.17, 123.85, 123.12, 120.06, 116.20, 113.30, 60.70, 53.75, 38.96; ESI-MS: m/z Calculated 613.46, found $[M+H]^+$ 614.4; Anal. Calcd for $C_{31}H_{22}Cl_2N_6O_4$: C, 60.70; H, 3.61; Cl, 11.56; N, 13.70; O, 10.43%; found C, 60.62; H, 3.37; N, 13.49%.

***2.3.18. N'-(2-(2-(4-bromophenyl)-5'-chloro-2'-oxo-1,10b-dihydrospiro[benzo[e] pyrazolo[1,5-c][1,3]oxazine-5,3'-indolin]-1'-yl)-2-oxoethyl)isonicotinohydrazide* (6ac):**

Dark brown solid; IR (KBr) (υmax, cm^{-1}): 3275 (C-H Aromatic), 1610 ($C=N_{str}$), 1770 ($C=O_{str}$), 1213 (C-O ether); ^{1}H NMR (400 MHz, DMSO) δ 9.06 - 8.93 (m, 2H), 8.91 (s, 1H), 7.99 - 7.81 (m, 2H), 7.70 (s, 1H), 7.54 - 7.30 (m, 7H), 7.27 (s, 1H), 7.12 (s, 1H), 6.99 (s, 1H), 5.18 (s, 1H), 4.90 (s, 1H), 3.85 (s, 1H), 3.73 (s, 1H), 2.67 (s, 1H), 2.42 (s, 1H); ^{13}C NMR (100 MHz, DMSO) δ 175.32, 167.84, 164.23, 154.15, 150.99, 145.86, 143.98, 139.99, 136.05, 134.33, 131.98, 131.57, 130.29, 127.52, 126.25, 123.85, 123.12, 121.78, 120.06, 116.20, 113.30, 60.70, 53.75,

38.96; ESI-MS: m/z Calculated 657.91, found $[M+H]^+$ 658.9; Anal. Calcd for $C_{31}H_{22}BrClN_6O_4$: C, 56.59; H, 3.37; Br, 12.15; Cl, 5.39; N, 12.77; O, 9.73%; found C, 56.22; H, 3.15; N, 12.42%.

***2.3.19. N'-(2-(2-(4-aminophenyl)-5'-chloro-2'-oxo-1,10b-dihydrospiro[benzo[e] pyrazolo[1,5-c][1,3]oxazine-5,3'-indolin]-1'-yl)-2-oxoethyl)isonicotinohydrazide* (6ad):**

Olive green solid; IR (KBr) (υmax, cm^{-1}): 3125 (C-H Aromatic), 1616 ($C=N_{str}$), 1778 ($C=O_{str}$), 1204 (C-O ether); ^1H NMR (400 MHz, DMSO) δ 8.95 (d, *J* = 7.4 Hz, 2H), 8.20 (s, 1H), 7.88 (d, *J* = 7.4 Hz, 2H), 7.62 (d, *J* = 1.3 Hz, 1H), 7.46 - 7.31 (m, 5H), 7.27 (td, *J* = 7.5, 1.5 Hz, 1H), 7.12 (td, *J* = 7.5, 1.5 Hz, 1H), 7.00 (dd, *J* = 7.5, 1.4 Hz, 1H), 6.64 (d, *J* = 7.5 Hz, 2H), 5.48 (s, 2H), 5.35 (t, *J* = 9.2 Hz, 1H), 3.82 (s, 1H), 3.73 (s, 1H), 3.53 (s, 1H), 2.67 (dd, *J* = 12.4, 9.1 Hz, 1H), 2.42 (dd, *J* = 12.4, 9.1 Hz, 1H); ^{13}C NMR (100 MHz, DMSO) δ 175.32, 167.84, 164.23, 154.15, 150.99, 147.40, 145.86, 143.98, 139.99, 136.05, 134.33, 130.29, 127.52, 126.93, 126.17, 123.85, 123.12, 122.22, 120.06, 116.20, 113.58, 113.30, 60.70, 53.75, 38.96; ESI-MS: m/z Calculated 594.03, found $[M+H]^+$ 595.0; Anal. Calcd for $C_{31}H_{24}ClN_7O_4$: C, 62.68; H, 4.07; Cl, 5.97; N, 16.51; O, 10.77%; found C, 62.34; H, 4.14; N, 16.97%.

***2.3.20. N'-(2-(5'-chloro-2-(4-hydroxyphenyl)-2'-oxo-1,10b-dihydrospiro[benzo[e]pyrazolo[1,5-c][1,3]oxazine-5,3'-indolin]-1'-yl)-2-oxoethyl)isonicotino hydrazide* (6ae):**

Saddle Brown solid; IR (KBr) (υmax, cm^{-1}): 3136 (C-H Aromatic), 1615 ($C=N_{str}$), 1749 ($C=O_{str}$), 1299 (C-O ether); ^1H NMR (400 MHz, DMSO) δ 8.93 (d, *J* = 7.4 Hz, 2H), 8.67 (s, 1H), 8.35 (s, 1H), 7.88 (d, *J* = 7.4 Hz, 2H), 7.71 (d, *J* = 7.5 Hz, 1H), 7.60 - 7.44 (m, 2H), 7.30 (qd, *J* = 7.8, 1.6 Hz, 4H), 7.14 (td, *J* = 7.5, 1.5 Hz, 1H), 6.91 - 6.68 (m, 3H), 5.00 (t, *J* = 9.1 Hz, 1H), 4.39 (s, 1H), 3.61 (s, 1H), 3.21 (s, 1H), 2.67 (dd, *J* = 12.4, 9.1 Hz, 1H), 2.42 (dd, *J* = 12.4, 9.1 Hz, 1H); ^{13}C NMR (100 MHz, DMSO) δ 175.32, 167.84, 164.23, 159.08, 154.15, 150.99, 145.86, 143.98, 139.99, 136.05, 134.33, 130.29, 128.09, 127.52, 126.17, 124.84, 123.85, 123.12, 120.06, 116.20, 115.78, 113.30, 60.70, 53.75, 38.96; ESI-MS: m/z Calculated 595.01, found $[M+H]^+$ 596.01; Anal. Calcd for $C_{31}H_{23}ClN_6O_5$: C, 62.58; H, 3.90; Cl, 5.96; N, 14.12; O, 13.44%; found C, 62.20; H, 3.40; N, 14.28%.

***2.3.21. N'-(2-(5'-chloro-2'-oxo-2-(p-tolyl)-1,10b-dihydrospiro[benzo[e]pyrazolo[1,5-c][1,3] oxazine-5,3'-indolin]-1'-yl)-2-oxoethyl)isonicotinohydrazide* (6af):**

Saddle Brown solid; IR (KBr) (υmax, cm^{-1}): 3255 (C-H Aromatic), 1620 ($C=N_{str}$), 1786 ($C=O_{str}$), 1241 (C-O ether); ^1H NMR (400 MHz, DMSO) δ 13.94 (s, 1H), 8.95 (d, *J* = 7.4 Hz, 2H), 7.88 (d, *J* = 7.2 Hz, 2H), 7.63 (dd, *J* = 4.4, 3.1 Hz, 2H), 7.55 - 7.35 (m, 4H), 7.31 (td, *J* = 7.5, 1.5 Hz, 1H), 7.21 (dd, *J* = 7.5, 1.5 Hz, 1H), 7.19 - 7.10 (m, 3H), 5.08 (t, *J* = 9.2 Hz, 1H), 3.93 (s, 1H), 3.65 (d, *J* = 17.2 Hz, 2H), 2.67 (dd, *J* = 12.4, 9.1 Hz, 1H), 2.42 (dd, *J* = 12.4, 9.1 Hz, 1H), 2.28 (s, 3H); ^{13}C NMR (100 MHz, DMSO) δ 175.32, 167.84, 164.23, 154.15, 150.99, 145.86, 143.98, 139.99, 139.17, 136.05, 134.33, 131.77, 130.29, 128.97, 127.52, 126.17, 125.43, 123.85, 123.12, 120.06, 116.20, 113.30, 60.70, 53.75, 38.96, 21.12; ESI-MS: m/z Calculated 593.04, found $[M+H]^+$ 594.0; Anal. Calcd for $C_{32}H_{25}ClN_6O_4$: C, 64.81; H, 4.25; Cl, 5.98; N, 14.17; O, 10.79%; found C, 64.43; H, 4.47; N, 14.56%.

***2.3.22. N'-(2-(5'-chloro-2-(4-fluorophenyl)-2'-oxo-1,10b-dihydrospiro[benzo[e] pyrazolo[1,5-c][1,3]oxazine-5,3'-indolin]-1'-yl)-2-oxoethyl)isonicotinohydrazide* (6ag):**

Greenish Brown solid; IR (KBr) (υmax, cm^{-1}): 3230 (C-H Aromatic), 1625 ($C=N_{str}$), 1727 ($C=O_{str}$), 1265 (C-O ether); ^1H NMR (400 MHz, DMSO) δ 8.95 (d, *J* = 7.4 Hz, 2H), 8.69 (s, 1H), 7.81 (d, *J* = 7.4 Hz, 2H), 7.68 (d, *J* = 7.5 Hz, 1H), 7.61 (d, *J* = 1.4 Hz, 1H), 7.44 (ddd, *J* = 7.5, 5.0, 1.3 Hz, 2H), 7.41 - 7.17 (m, 3H), 7.11 (td, *J* = 7.5, 1.4 Hz, 1H), 7.05 - 6.92 (m, 3H), 5.00 (t, *J* = 9.1 Hz, 1H), 4.71 (s, 1H), 3.97 (s, 1H), 3.76 (s, 1H), 2.67 (dd, *J* = 12.4, 9.1 Hz, 1H), 2.42 (dd, *J* = 12.4, 9.1 Hz, 1H); ^{13}C NMR (100 MHz, DMSO) δ 175.32, 167.84, 164.23, 163.10, 160.48, 154.15, 150.99, 145.86, 143.98, 139.99, 136.05, 134.33, 130.29, 129.28, 128.32, 127.52, 126.17, 123.85, 123.12, 120.06, 116.37, 113.30, 60.70, 53.75, 38.96; ESI-MS: m/z Calculated 597.00, found $[M+H]^+$ 598.0; Anal. Calcd for $C_{31}H_{22}ClFN_6O_4$: C, 62.37; H, 3.71; Cl, 5.94; F, 3.18; N, 14.08; O, 10.72%; found C, 62.64; H, 3.44; N, 14.19%.

***2.3.23. N'-(2-(2-(3-bromophenyl)-5'-chloro-2'-oxo-1,10b-dihydrospiro[benzo[e]pyrazolo[1,5-c][1,3]oxazine-5,3'-indolin]-1'-yl)-2-oxoethyl)isonicotinohydrazide* (6ah):**

Saddle Brown solid; IR (KBr) (υmax, cm^{-1}): 3055 (C-H Aromatic), 1616 ($C=N_{str}$), 1730 ($C=O_{str}$), 1175 (C-O ether); ^1H NMR (400 MHz, DMSO) δ 8.96 (d, *J* = 7.4 Hz, 2H), 8.76 (s, 1H), 7.90 (d, *J* = 7.4 Hz, 2H), 7.77 (t, *J* = 1.4 Hz, 1H), 7.66 (d, *J* = 1.5 Hz, 1H), 7.54 (d, *J* = 7.5 Hz, 1H), 7.45 (ddt, *J* = 7.4, 4.6, 1.2 Hz, 3H), 7.32 (dd, *J* = 7.4, 1.5 Hz, 1H), 7.26 (td, *J* = 7.5, 1.6 Hz, 1H), 7.19 (t, *J* = 7.4 Hz, 1H), 7.10 (td, *J* = 7.5, 1.4 Hz, 1H), 6.98 (dd, *J* = 7.4, 1.5 Hz, 1H), 5.17 (t, *J* = 5.8 Hz, 1H), 4.00 (s, 1H), 3.88 (s, 1H), 3.75 (s, 1H), 2.67 (dd, *J* = 12.4, 5.8 Hz, 1H), 2.42 (dd, *J* = 12.4, 5.8 Hz, 1H); ^{13}C NMR (100 MHz, DMSO) δ 175.32, 167.84, 164.23, 154.15, 150.99, 145.08, 143.98, 139.99, 136.05, 134.66, 134.33, 130.29, 130.05, 129.80, 127.61, 126.17, 124.63, 123.85, 123.12, 120.06, 116.20, 113.30, 60.70, 53.75, 38.96; ESI-MS: m/z Calculated 657.91, found $[M+H]^+$ 658.9; Anal. Calcd for $C_{31}H_{22}BrClN_6O_4$: C, 56.59; H, 3.37; Br, 12.15; Cl, 5.39; N, 12.77; O, 9.73%; found C, 56.46; H, 3.96; N, 12.41%.

***2.3.24. N'-(2-(5'-chloro-2-(4-nitrophenyl)-2'-oxo-1,10b-dihydrospiro[benzo[e]pyrazolo[1,5-c][1,3]oxazine-5,3'-indolin]-1'-yl)-2-oxoethyl)isonicotinohydrazide* (6ai):**

Saddle Brown solid; IR (KBr) (υmax, cm^{-1}): 3152 (C-H Aromatic), 1632 ($C=N_{str}$), 1761 ($C=O_{str}$), 1085 (C-O ether); ^1H NMR (400 MHz, DMSO) δ 8.96 (d, *J* = 7.4 Hz, 2H), 8.60 (s, 1H), 8.19 (d, *J* = 7.5 Hz, 2H), 7.89 (dd, *J* = 12.6, 7.5 Hz, 3H), 7.73 (d, *J* = 7.5 Hz, 2H), 7.63 (d, *J* = 1.6 Hz, 1H), 7.53 (dd, *J* = 7.5, 1.6 Hz, 1H), 7.32 (dd, *J* = 7.4, 1.5 Hz, 1H), 7.25 (td, *J* = 7.5, 1.5 Hz, 1H), 7.10 (td, *J* = 7.5, 1.4 Hz, 1H), 7.05 - 6.87 (m, 1H), 5.09 (t, *J* = 9.1 Hz, 1H), 3.96 (s, 1H), 3.69 (s, 1H), 3.36 (s, 1H), 2.67 (dd, *J* = 12.4, 9.1 Hz, 1H), 2.42 (dd, *J* = 12.4, 9.1 Hz, 1H); ^{13}C NMR (100 MHz, DMSO) δ 175.32, 167.84, 164.23, 154.15, 150.99, 146.30, 145.86, 143.98, 139.99, 136.93, 136.05, 134.33, 130.29, 127.52, 126.17, 125.51, 123.85, 123.12, 120.06, 116.20, 113.30, 60.70, 53.75, 38.96; ESI-MS: m/z Calculated 624.01, found $[M+H]^+$ 625.0; Anal. Calcd for $C_{31}H_{22}ClN_7O_6$: C, 59.67; H, 3.55; Cl, 5.68; N, 15.71; O, 15.38%; found C, 59.54; H, 3.24; N, 15.34%.

***2.3.25. N'-(2-(5'-chloro-2-(2-hydroxyphenyl)-2'-oxo-1,10b-dihydrospiro[benzo [e]pyrazolo[1,5-c][1,3]oxazine-5,3'-indolin]-1'-yl)-2-oxoethyl)isonicotino hydrazide* (6aj):**

Sienna Brown solid; IR (KBr) (υmax, cm^{-1}): 3251 (C-H Aromatic), 1684 ($C=N_{str}$), 1727 ($C=O_{str}$), 1140 (C-O ether); ^1H NMR (400 MHz, DMSO) δ 11.13 (s, 1H), 8.93 (d, *J* = 7.4 Hz, 2H), 8.33 (s,

1H), 7.84 (d, *J* = 7.4 Hz, 2H), 7.71 (d, *J* = 1.6 Hz, 1H), 7.65 (d, *J* = 7.5 Hz, 1H), 7.45 (dd, *J* = 7.5, 1.4 Hz, 1H), 7.43 - 7.21 (m, 3H), 7.13 (td, *J* = 7.5, 1.5 Hz, 1H), 7.07 (td, *J* = 7.5, 1.6 Hz, 1H), 7.04 - 6.91 (m, 2H), 6.85 (dd, *J* = 7.4, 1.5 Hz, 1H), 5.74 (t, *J* = 5.4 Hz, 1H), 5.61 (s, 1H), 4.18 (s, 1H), 3.69 - 3.50 (m, 2H), 2.42 (dd, *J* = 12.4, 5.4 Hz, 1H); ^{13}C NMR (100 MHz, DMSO) δ 175.32, 167.84, 164.23, 157.79, 154.15, 150.99, 143.98, 139.99, 138.27, 136.05, 134.33, 130.29, 129.84, 127.8, 127.52, 126.17, 123.85, 123.12, 121.25, 120.06, 118.65, 116.20, 115.54, 113.30, 60.70, 53.75, 38.89; ESI-MS: m/z Calculated 595.01, found $[M+H]^+$ 596.0; Anal. Calcd for $C_{31}H_{23}ClN_6O_5$: C, 62.58; H, 3.90; Cl, 5.96; N, 14.12; O, 13.44%; found C, 62.44; H, 3.40; N, 14.37%.

***2.3.26. N'-(2-(5'-chloro-2-(4-methoxyphenyl)-2'-oxo-1,10b-dihydrospiro[benzo[e]pyrazolo [1,5-c][1,3]oxazine-5,3'-indolin]-1'-yl)-2-oxoethyl)isonicotinohydrazide* (6ak):**

Saddle Brown solid; IR (KBr) (υmax, cm^{-1}): 3155 (C-H Aromatic), 1641 ($C=N_{str}$), 1737 ($C=O_{str}$), 1243 (C-O ether); ^{1}H NMR (400 MHz, DMSO) δ 8.95 (d, *J* = 7.4 Hz, 2H), 8.73 (s, 1H), 7.91 (d, *J* = 7.4 Hz, 2H), 7.73 (d, *J* = 7.5 Hz, 1H), 7.66 (d, *J* = 1.4 Hz, 1H), 7.58 - 7.41 (m, 3H), 7.41 - 7.20 (m, 2H), 7.07 (td, *J* = 7.5, 1.4 Hz, 1H), 7.04 - 6.82 (m, 3H), 5.26 (t, *J* = 6.2 Hz, 1H), 4.10 (d, *J* = 19.4 Hz, 2H), 3.84 (s, 1H), 3.78 (s, 3H), 2.67 (dd, *J* = 12.5, 6.2 Hz, 1H), 2.42 (dd, *J* = 12.3, 6.2 Hz, 1H); ^{13}C NMR (100 MHz, DMSO) δ 175.32, 167.84, 164.23, 159.72, 154.15, 150.99, 145.86, 143.98, 139.99, 136.05, 134.33, 130.29, 127.42, 126.78, 126.17, 123.85, 123.12, 120.06, 116.20, 114.84, 113.30, 60.70, 56.03, 53.75, 38.96; ESI-MS: m/z Calculated 609.04, found $[M+H]^+$ 610.0; Anal. Calcd for $C_{32}H_{25}ClN_6O_5$: C, 63.11; H, 4.14; Cl, 5.82; N, 13.80; O, 13.13%; found C, 63.33; H, 4.34; N, 13.46%.

***2.3.27. N'-(2-(5'-chloro-2-(2-chlorophenyl)-2'-oxo-1,10b-dihydrospiro[benzo[e]pyrazolo[1,5-c] [1,3]oxazine-5,3'-indolin]-1'-yl)-2-oxoethyl)isonicotinohydrazide* (6al):**

Saddle Brown solid; IR (KBr) (υmax, cm^{-1}): 3200 (C-H Aromatic), 1670 ($C=N_{str}$), 1676 ($C=O_{str}$), 1260 (C-O ether); ^{1}H NMR (400 MHz, DMSO) δ 8.93 (d, *J* = 7.4 Hz, 2H), 8.21 (s, 1H), 7.83 (d, *J* = 7.4 Hz, 2H), 7.60 (d, *J* = 1.3 Hz, 1H), 7.52 - 7.23 (m, 6H), 7.18 - 7.08 (m, 3H), 6.98 (dd, *J* = 7.4, 1.5 Hz, 1H), 5.01 (t, *J* = 9.1 Hz, 1H), 3.92 (d, *J* = 9.0 Hz, 2H), 3.79 (s, 1H), 2.67 (dd, *J* = 12.4, 9.1 Hz, 1H), 2.42 (dd, *J* = 12.4, 9.1 Hz, 1H); ^{13}C NMR (100 MHz, DMSO) δ 175.32, 167.84, 164.23, 154.15, 150.99, 144.48, 143.98, 139.99, 136.05, 134.33, 133.42, 131.78, 130.20, 127.82, 127.52, 126.84, 126.17, 123.85, 123.12, 120.06, 116.20, 113.30, 60.70, 53.75, 38.89; ESI-MS: m/z Calculated 613.46, found $[M+H]^+$ 614.4; Anal. Calcd for $C_{31}H_{22}Cl_2N_6O_4$: C, 60.70; H, 3.61; Cl, 11.56; N, 13.70; O, 10.43%; found C, 60.50; H, 3.64; N, 13.58%.

***2.3.28. N'-(2-(5'-chloro-2-(3-nitrophenyl)-2'-oxo-1,10b-dihydrospiro[benzo[e]pyrazolo[1,5-c] [1,3]oxazine-5,3'-indolin]-1'-yl)-2-oxoethyl)isonicotinohydrazide* (6am):**

Dark brown solid; IR (KBr) (υmax, cm^{-1}): 3241 (C-H Aromatic), 1691 ($C=N_{str}$), 1800 ($C=O_{str}$), 1271 (C-O ether); ^{1}H NMR (400 MHz, DMSO) δ 8.89 (d, *J* = 7.4 Hz, 2H), 8.57 (t, *J* = 1.4 Hz, 1H), 8.17 (dt, *J* = 7.5, 1.5 Hz, 1H), 8.01 (s, 1H), 7.95 - 7.74 (m, 3H), 7.64 (dd, *J* = 16.4, 4.4 Hz, 2H), 7.56 (t, *J* = 7.5 Hz, 1H), 7.40 (ddd, *J* = 11.0, 7.5, 1.4 Hz, 2H), 7.25 (td, *J* = 7.5, 1.5 Hz, 1H), 7.09 (td, *J* = 7.5, 1.4 Hz, 1H), 6.97 (dd, *J* = 7.5, 1.4 Hz, 1H), 5.96 (t, *J* = 6.0 Hz, 1H), 5.28 (s, 1H), 4.30 (s, 1H), 3.69 (s, 1H), 2.67 (dd, *J* = 12.4, 6.1 Hz, 1H), 2.42 (dd, *J* = 12.5, 6.0 Hz, 1H);

^{13}C NMR (100 MHz, DMSO) δ 175.32, 167.84, 164.23, 154.15, 150.99, 147.74, 145.08, 143.98, 139.99, 136.05, 135.81, 134.33, 130.36, 129.29, 127.52, 126.17, 124.10, 123.85, 123.12, 121.84, 120.06, 116.20, 113.30, 60.70, 53.75, 38.96; ESI-MS: m/z Calculated 624.01, found $[M+H]^+$ 625.0; Anal. Calcd for $C_{31}H_{22}ClN_7O_6$: C, 59.67; H, 3.55; Cl, 5.68; N, 15.71; O, 15.3 %; found C, 59.56; H, 3.26; N, 15.34%.

***2.3.29. N'-(2-(5'-chloro-2-(2,4-dichlorophenyl)-2'-oxo-1,10b-dihydrospiro[benzo[e]pyrazolo [1,5-c][1,3]oxazine-5,3'-indolin]-1'-yl)-2-oxoethyl)isonicotinohydrazide* (6an):**

Olive green solid; IR (KBr) (υmax, cm^{-1}): 3245 (C-H Aromatic), 1645 ($C=N_{str}$), 1690 ($C=O_{str}$), 1200 (C-O ether); ^{1}H NMR (400 MHz, DMSO) δ 8.95 (d, *J* = 7.4 Hz, 2H), 8.48 (s, 1H), 7.90 (d, *J* = 7.4 Hz, 2H), 7.71 (d, *J* = 7.5 Hz, 1H), 7.63 (d, *J* = 1.4 Hz, 1H), 7.44 (dd, *J* = 7.8, 1.8 Hz, 1H), 7.43 - 7.31 (m, 3H), 7.31 - 7.13 (m, 2H), 7.11 (td, *J* = 7.5, 1.5 Hz, 1H), 6.98 (dd, *J* = 7.5, 1.4 Hz, 1H), 5.58 (t, *J* = 9.0 Hz, 1H), 4.47 (s, 1H), 4.08 (s, 1H), 3.80 (s, 1H), 2.74 - 2.65 (m, 1H), 2.44 - 2.36 (m, 1H); ^{13}C NMR (100 MHz, DMSO) δ 175.32, 167.84, 164.23, 154.15, 150.99, 144.48, 143.98, 139.99, 136.05, 134.33, 133.42, 132.99, 132.69, 130.55, 130.29, 128.41, 127.86, 127.52, 126.17, 123.85, 123.12, 120.06, 116.20, 113.30, 60.70, 53.75, 38.89; ESI-MS: m/z Calculated 647.90, found $[M+H]^+$ 648.9; Anal. Calcd for $C_{31}H_{21}Cl_3N_6O_4$: C, 57.47; H, 3.27; Cl, 16.41; N, 12.97; O, 9.88%; found C, 57.67; H, 3.47; N, 12.46%.

***2.3.30. N'-(2-(5'-chloro-2-(2-methoxyphenyl)-2'-oxo-1,10b-dihydrospiro[benzo[e]pyrazolo[1,5-c][1,3]oxazine-5,3'-indolin]-1'-yl)-2-oxoethyl)isonicotinohydrazide* (6ao):**

Saddle Brown solid; IR (KBr) (υmax, cm^{-1}): 3260 (C-H Aromatic), 1630 ($C=N_{str}$), 1763($C=O_{str}$), 1089 (C-O ether); ^{1}H NMR (400 MHz, DMSO) δ 10.72 (s, 1H), 9.05 - 8.86 (m, 2H), 8.02 - 7.83 (m, 2H), 7.73 (s, 1H), 7.67 (s, 1H), 7.48 (d, *J* = 30.2 Hz, 2H), 7.30 (s, 1H), 7.24 (d, *J* = 1.2 Hz, 2H), 7.07 (s, 1H), 6.97 (d, *J* = 0.5 Hz, 2H), 6.90 (s, 1H), 5.25 (s, 1H), 4.20 (s, 1H), 4.08 (s, 1H), 3.82 - 3.77 (m, 3H), 3.73 (s, 1H), 2.67 (s, 1H), 2.42 (s, 1H); ^{13}C NMR (100 MHz, DMSO) δ 175.32, 167.84, 164.23, 158.35, 154.15, 150.99, 143.98, 139.99, 136.73, 136.05, 134.33, 130.29, 128.31, 127.52, 127.27, 126.17, 123.77, 123.12, 121.85, 120.06, 116.20, 114.88, 113.30, 60.70, 56.78, 53.75, 38.89; ESI-MS: m/z Calculated 609.04, found $[M+H]^+$ 610.0; Anal. Calcd for $C_{32}H_{25}ClN_6O_5$: C, 63.11; H, 4.14; Cl, 5.82; N, 13.80; O, 13.13%; found C, 63.40; H, 4.25; N, 13.40%.

2.4. Antimycobacterial activity

2.4.1. Method 1: Lowenstein-Jensen (L-J) method for the zone of inhibition

All the newly synthesized compounds **(6a-6ao)** were screened for their *in vitro* antimycobacterial activity against *Mycobacterium tuberculosis* H_{37}Rv using Lowenstein-Jensen (L-J) method. The anti-mycobacterial assay was performed in the L-J medium. An antibiotic standard used was isoniazid. Determination of Colony-forming units (c.f.u) on L-J in brief, the ten-fold dilution of standard 1 mg/mL, *M. tuberculosis* suspension[26] were streaked on L-J medium for determining c.f.u in the presence and absence of compound. An M. tuberculosis suspension of 1 mg/ml is equivalent to the MacFarland standard.[27] One loopful (6 µl) of this suspension was streaked on the L-J slants using a 3 mm external diameter loop. Reagents of L-J media included potassium dihydrogen phosphate anhydrous (Qualigens), magnesium sulfate

anhydrous (Qualigens), magnesium citrate (Loba Chemie), L-asparagine (Hi-media, Mumbai), glycerol (Fisher Scientific, Mumbai), and malachite green (Hi-Media, Mumbai). The drug was incorporated in the medium at a concentration of 2 percent v/v and 4 percent v/v of the drug was dissolved into 100 ml of culture medium prior to inspissation. The medium set inoculated with the standard bacterial suspension and incubated at 37 °C for 42 days. Reading was taken weekly. For comparison, drug-free control slants were used. Susceptibility testing of $H_{37}Rv$ isolates was also performed against standard drugs like isoniazid. Each test was done in triplicate. Percentage inhibition was calculated by the mean reduction in the number of colonies on drug-containing as compared to drug-free controls.

$$\% \text{ inhibition} = \frac{Cc - Ct}{Cc} X\ 100$$

Where, c = control, t = test.

2.4.2. Method 2: Lowenstein–Jensen (L-J) method for MIC value

Drug susceptibility and determination of MIC of the test compounds **(6a-6ao)** against *Mycobacterium tuberculosis* $H_{37}Rv$ were performed by Lowenstein-Jensen (L-J) MIC method.[28,29] Where primary 1000, 500, 250, and secondary 200, 100, 62.5, 50, 25, 12.5, 6.25, 3.25 µg mL^{-1} dilutions of each test compound was added to liquid Lowenstein–Jensen medium. The standard strain *M. tuberculosis* $H_{37}Rv$ was tested with known drug isoniazid. Further, compounds **6a**, **6b**, **6e**, **6g**, **6h**, **6o**, **6ab**, **6ad**, and **6ag** were tested for MDR-TB.

2.5. Statistical analysis

The determination assay for each Antimycobacterial activity result was carried out in thrice to minimize the percentage of error. Statistical analysis was performed using the Statistical Package for Social Science (IBM SPSS Statistics 20 for Windows, SPSS Inc., Chicago, IL, USA).

2.6. In silico ADMET properties

In silico pharmacokinetic properties and toxicities were predicted using Accelrys Discovery Studio 2.1. All the compounds were prepared in neutralized form for the calculation of pharmacokinetic properties by the Marvin Suite program saved in SD format. The module uses six mathematical models, to predict properties quantitatively by a set of keys **(Table 1)** that specify threshold ADMET characteristics for the chemical structure of the molecules based on available drug information. For the ADMET human intestinal absorption[6], the model was developed using 199 compounds in the training set based on the calculations AlogP (ADMET_AlogP98) and polar surface area (PSA_2D). ADMET aqueous solubility predicts the solubility of all compounds in water at 25 °C. The model is based on a genetic partial least squares method on a training set of 784 compounds with experimentally measured solubilities.[30] ADMET Blood-Brain Barrier (BBB) model predicts blood-brain penetration of a molecule after oral administration. This model was derived from a quantitative linear regression model, over 800 compounds that are known to enter the CNS after oral administration.[31] ADMET Plasma Protein Binding (PPB) model predicts whether a compound is likely to be

highly bound to carrier proteins in the blood. Binding levels predicted by the marker similarities are modified according to conditions on calculated logP [32] ADMET CYP2D6 binding predicts cytochrome P4502D6 enzyme inhibition using the 2D chemical structure as input and a probable estimate for the prediction. Predictions are based on a training set of 100 compounds with known CYP2D6 inhibitions.[33] ADMET hepatotoxicity predicts the potential human hepatotoxicity for a varied range of structurally different compounds. Predictions are based on a model of 382 training compounds known to exhibit liver toxicity or to trigger dose-related elevated aminotransferase levels in more than 10% of the human population.[34]

2.7. Molecular Docking

Molecular docking and Molecular dynamics were performed using the YASARA (Yet Another Scientific Artificial Reality Application) commercial package. The experiments were accomplished using Autodock Vina 1.0 [35] configured in YASARA Structure [36] with eight central processing units in a Microsoft Windows™ workstation equipped with Intel® Xeon™ E5620 processor. Docking analysis is a significant step for the selection of potential hits in virtual screening. Consequently, grid points with 0.35 Å spacing were enumerated using Autodock Vina default optimization parameters. The experimentally verified active site residues were demarcated as a docking area. The torsional angles of the ligands and active site residues side chains have been made flexible due to obtain a favorable binding conformation. For considering standard docking procedure, 100 genetic algorithm runs per ligand with an initial population of 150 randomly placed individually. The maximum number of energy evaluations was limited to 2.5×10^5. The rate of gene mutation and crossover was controlled to 0.02 and 0.8. The docking poses from each experiment (100 solutions) were gathered on the basis of docking energy (kcal/mol) and the root mean squared deviation (RMSD). The most noticeable thing is that higher positive energies mean better binding, and negative energies mean no binding according to YASARA energy parameters. The docking energy was calculated by the following equation.

$$\Delta G = \Delta G_{vdw} + \Delta G_{Hbond} + \Delta G_{elec} + \Delta G_{tor} + \Delta G_{desolv}$$

Where, ΔG_{vdw} = van der Waals term for docking energy
ΔG_{Hbond} = H bonding term for docking energy
ΔG_{elec} = electrostatic term for docking energy
ΔG_{tor} = torsional free energy term for ligand when the ligand transits from unbounded to bounded state
ΔG_{desolv} = desolvation term for docking energy

2.7.1. Preparation of Ligands

Three-dimensional structures of ligand input for all docking experiments were generated using the Marvin Suite applications (Marvin Sketch) followed by adding explicit hydrogen with cleaning, energy minimization, and alignment process. The generated structures were saved as MOL2/SDF files by energy minimization using the MMFF94 force field.

2.7.2. Preparation of Receptors

To investigate the ligand-protein interactions of synthesized compounds, docking studies were performed on all compounds against isoniazid-resistant I21V enoyl-ACP(COA) reductase mutant enzyme from *Mycobacterium tuberculosis* in Complex with NADH-INH (PDB entry: 2IE0)[37] Crystal structure of 2IE0 was retrieved from RCSB Protein Data Bank (http://www.pdb.org). The structure having the depth of resolution 2.2 Å, crystal structure includes Oxidoreductase enzyme 268 amino acids chain length, ligand placed isonicotinic-acetyl-nicotinamide-adenine dinucleotide (ZID) which are effective in recognition of its active binding sites. The 3D structures determined by X-ray diffraction of *Escherichia coli* (PDB ID: 2IE0). The protein structure was treated using standard molecular mechanics protocol which includes removal of crystallographic waters, the addition of polar hydrogens, assignment of bond orders, and Kollman charge [38]. The protein structure with bound isonicotinic-acetyl-nicotinamide-adenine dinucleotide was atom-typed with the Amber03 force field [39] and energy minimized using steepest descent technique (100 iterations) in YASARA Structure program.[36] The interaction profiles for all generated hits have been studied. The active side of amino acid residues was determined which is being used to dock molecules for automated docking and scoring. The active site residues of the enoyl-ACP(COA) reductase enzyme are Ile194, Gly96, Trp222, Gly14, Lys165, Tyr158, Asp64, Val21, Met147, Pro193, Leu63, Phe41, Ala191, Phe149, Ser94, Ile122, Met199, Ile95, Val65, Thr196, Asp148, Gly192, Ile15, Ser20, Ile16.

2.8. Molecular Dynamics

The residence time and binding stability of the designed ligands in complex with isoniazid-resistant enoyl-ACP (COA) reductase mutant enzyme from *Mycobacterium Tuberculosis* were examined using molecular dynamic simulations. The dock poses of these receptor-ligand complexes were energy minimized due to remove unfavorable atomic contacts and subsequently specified as starting conformation for dynamic simulations in YASARA structure software. [36] The hydrogen-bonding network in the complexes was optimized as well as atom typed using the AMBER03 force field [36] intended for its application in aqueous solution. The acid dissociation constant (pKa) values of titratable amino acids were assigned and chosen orthorhombic simulation box with other default parameters of periodic boundary conditions. molecular dynamics simulation were performed by following steps: the temperature at 298 K, pressure of 1 bar, pH 7.0, coulomb electrostatics at a cutoff of 7.86, solvated by water model (density 0.997 gL^{-1}) inside the simulation cell, 0.9 % as ion concentration of NaCl to neutralize the system and to minimize the energy using steepest gradient approach (100 cycles) and all atoms were mobile. The 2IE0 protein was cleaned, hydrogens were added and water molecules were removed. 10 ns production time had been chosen for the analysis of protein structure evaluations by every 2500 ps. The generated time trajectories of the selected protein-ligand complex were analyzed for the stabilization of protein viz. RMSD parameter. The protein-ligand interaction patterns of protein-ligand complex generated at the starting time and ending time through the Protein-Ligand Interaction Profiler server. The average structures were determined from the simulations and were used to calculate the RMSDs for the respective model.

3. Results and discussion

3.1. Chemistry

The molecular hybridization is a strategy of rational drug design of new ligands or prototypes based on the recognition of pharmacophoric sub-unities in the molecular structure of two or more known bioactive derivatives which, through the adequate fusion of these sub-unities, lead to the design of new hybrid architectures that maintain pre-selected characteristics of the original templates. Furthermore, this strategy can result in compounds presenting modified selectivity profiles, different and/or dual modes of action, and reduced undesired side effects. In our previous work(*25*), we have reported synthesis of five compound series of 2-phenyl-1,10bdihydrospiro [benzo[e]Pyrazolo[1,5-c][1,3]oxazine-5,3'-indolin]-2'-ones derivatives **(5a-5e)** by conventional as well as microwave methods. These compounds were showed good antimycobacterial activities. In an effort to prepare a better therapeutic agent for the treatment of tuberculosis and in continuation of our efforts, we have attempted to design novel antimycobacterial agents by hybridizing isoniazid linker to spirooxindole scaffold. Incorporation of two biologically versatile heterocyclic scaffolds like isoniazid and spirooxindole in a single molecular platform was undertaken. Therefore, the designed compound possessed two pharmacophoric units, Isoniazid, a linker stacked between spirooxindole core as shown in (Fig. 2).

A series of targeted compounds dihydrospiro[benzopyrazolo[1,5-c][1,3]oxazine-5,3'-indolin]isonicotinohydrazide derivatives **(6a-6ao)** were synthesized by stepwise reactions that have been demonstrated in **Scheme 1**. In the first step, we have described an efficient, one-pot synthesis of 2-phenyl-1,10b-dihydrospiro[benzo[e]Pyrazolo[1,5-c][1,3]oxazine-5,3'-indolin]-2'-ones **(5a-5ao)** by the reaction between 2-(3-(4-substituted phenyl)-4,5-dihydro-1*H*pyrazol-5-yl) phenol derivatives **(4a-4o)** and isatin derivative using *p*-TSA as a prompt catalyst under conventional as well as microwave methods, with better yield and short reaction time. In the next step, compound **(5a-5ao)** react with chloroacetyl chloride in the presence of triethylamine at 0°C temperature and followed by react with isoniazid to give *N*'-(2-oxo-2-(2'-oxo-2-phenyl-1,10b-dihydrospiro[benzo[e]pyrazolo [1,5-c][1,3]oxazine-5,3'-indolin]-1'-yl)ethyl)isonicotine hydrazide **(6a-6ao)** with good 60-80% practical yield. A comparison of yield and melting point for the synthesis of **6a-6ao** was mentioned in **Table 2**.

Designed series of isoniazid-spirooxindole derivatives **(6a-6ao)** were characterized by elemental analysis and different spectroscopic techniques like IR, ^{1}H NMR, ^{13}C NMR, and mass spectrometry and were in full agreement with proposed synthesized structures. The IR spectrum of **6a** exhibited four main peaks situated at 3255, 1616, 1724, and 1213 cm^{-1}, which were assigned to the ($C\text{-}H_{str}$) aromatic, ($C{=}N_{str}$) imine, ($C{=}O_{str}$) ketone, ($C\text{-}O_{str}$) ether respectively. The ^{1}H NMR spectrum of **6a** showed a singlet at 11.86 (s, 1H) δ value is due to amidic N-H proton of isoniazid. Another N-H proton of isoniazid gives singlet at 3.9 (s, 1H) δ ppm. Chiral carbon (C-H) of pyrazole ring displayed a triplet at δ 5.49 (t, J = 6.4 Hz, 1H) and two characteristic peaks of neighboring chemically non-equivalent, diastereotopic protons showed as double doublet at 2.42 (dd, J = 12.4, 6.4 Hz, 1H) and 2.67 (dd, J = 12.4, 6.4 Hz, 1H) δ ppm. All the protons of aromatic regions appeared in the range of 6.9 - 8.9 δ ppm. Sidechain contained pyridine ring's proton which resonates at 8.95 (d, J = 7.5 Hz, 2H), 7.95 (d, J = 7.2 Hz, 2H) δ ppm. The ^{13}C NMR spectrum of **6a** showed the carbonyl carbons of isatin, isoniazid, and the side

chain of isatin displays signals at 175, 164, and 167 ppm, correspondingly. The -CH and -CH_2 carbons of pyrazole ring resonated at 60 and 38.9 ppm, respectively. Another CH_2 carbon of isatin linkage showed a signal at 53 ppm. Values between 111-139 ppm are due to aromatic carbons present in all the aromatic rings in compound **6a**. Mass spectrum of **6a** gave a molecular ion peak at m/z 545.5 due to $[M+H]^+$ thereby confirming the structure. In compound **6a**, the characteristic peaks for protons and carbons in ^{1}H-NMR and ^{13}C-NMR appeared at specific chemical shift values were in good agreement with the molecular formula of the synthesized compounds.

3.2. In vitro antimycobacterial activity

Because of the increased resistance diversity of tuberculosis in contradiction of standard drugs, there is an urgent requirement for the development of novel drug moiety that could susceptibly kill *Mycobacterium* species. This approach was laid for the development of such compounds with increased efficiency in terms of lower MIC values to kill H_{37}Rv with a maximum percent inhibition. The synthesized isoniazid-spirooxindole derivatives **(6a-6ao)** have been evaluated for anti-tubercular activity against *Mycobacterium tuberculosis* H_{37}Rv as shown in **Table 3**, (Fig. 3). Compound **6ab** which has two chloro (-Cl) groups at the para position of a benzene ring and fifth position of isatin proves to be the best anti-tubercular agent (highest % inhibition value 81.88) shows MIC value 12.5 µg mL^{-1}. Compound **6a** (% inhibition 72.25), **6c** (% inhibition 76.30), **6f** (% inhibition 65.89), **6h** (% inhibition 71.09), **6l** (% inhibition 58.69), **6n** (% inhibition 52.89), **6af** (% inhibition 58.67), **6ai** (% inhibition 46.28), **6am** (% inhibition 46.28) and **6ao** (% inhibition 46.28), are known to show same MIC value (250 µg mL^{-1}) with variation in percent inhibition values of the targeted pathogenic strain of *Mycobacterium*. Compounds **6a** (R= 4-H), **6c** (R= 4-Br), **6g** (R= 4-F) and **6h** (R= 3-Br) were found to be more active in comparison to other compounds with %inhibition in the range of 70-77%. Compounds **6o** (R = 2-OCH_3) and **6ad** (R = 4-NH_2, R_1 = Cl) having electron-donating and electro withdrawing groups showed better antimycobacterial activity at MIC value 25 µg mL^{-1}. Compounds **6e** (R = 4-OH) and **6ag** (R = 4-F) also have good MIC value 62.5 µg mL^{-1}. Compounds **6g**, **6k**, **6ac**, **6ah**, **6an,** and **6ah** inhibit the *M.tuberculosis* at 100 µg mL^{-1} which displayed moderate to good activity. Compound **6a** (500 µg mL^{-1}), **6b** (500 µg mL^{-1}), **6e** (100 µg mL^{-1}), **6g** (125 µg mL^{-1}), **6h** (1000 µg mL^{-1}), **6o** (62.5 µg mL^{-1}), **6ab** (50 µg mL^{-1}), **6ad** (62.5 µg mL^{-1}), **6ag** (500 µg mL^{-1}) were to be screened for MDR-TB using Kanamycin (62.5 µg mL^{-1}) as a standard drug (**Table 4**). Out of them, compound **6ab** showed good MIC value 50 µg mL^{-1}. The presence of the isoniazid and spirooxindole ring as pharmacophores and different derivatives of acetophenone increase the lipophilic character of the molecule. The presence of electro donating and electro withdrawing groups on acetophenone and isatin derivative facilitates the crossing through the biological membrane of the microorganism thereby inhibiting their growth.

3.3. In silico ADMET Prediction and evaluation of Lipinski's 'Rule of 5'

ADME/Toxicity properties, pharmacokinetics, and toxicity are a major indication for the failure of drugs in the drug development process. Thus, the initial assessment of ADMET (Adsorption, Distribution, Metabolism, Excretion, and Toxicity) is necessary for an effective drug development process. We have predicted the ADMET properties of test compounds with reference compound isoniazid for the pharmaceutically relevant properties to evaluate the drug-

likeness and pharmacokinetic properties **(Table 5)**. In the theory of ADMET descriptors, various protocols generate models to evaluate the pharmacokinetic properties. Human Intestinal Absorption [6] model predicts human intestinal absorption after oral administration. A well-absorbed compound is one that is absorbed in least 90% into the bloodstream in humans. Isoniazid has good absorption than all the compounds. Compound **6a** and **6g** show moderate absorption, on the other hand, compounds **6i**, **6m**, **6ai** and **6am** showed very low absorption. Other compounds absorb very poorly. According to the model, a compound should have optimum cell permeability criteria (PSA < 140 $Å^2$ and AlogP98 < 5).[40] Most of the compounds showed a polar surface area (PSA) < 140 $Å^2$. Considering the AlogP98 criteria, all compounds had AlogP98 value <5, except four compounds. There was no blood-brain penetration of any compound is to be defined after oral administration because of the BBB (blood-brain barrier) level is 4. The aqueous solubility plays an important role in the bioavailability of the drug candidate. Categorical solubility level is extremely low of compound **6an** and also all of the other compounds than standard. Further, all compounds have been predicted to have a hepatotoxicity level of 1, except isoniazid. The hepatotoxicity model predicts potential organ toxicity for a wide range of structurally diverse compounds. Isoniazid is non-toxic and unlikely to cause dose-dependent liver injuries. Moreover, all the compounds are seemed to be toxic to the liver. ADMET CYP2D6, the model predicts cytochrome P4502D6 enzyme inhibition. Compounds **6m**, **6n**, **6ai**, **6aj**, **6al**, **6an,** and isoniazid are non-inhibitor and unlikely to inhibit the CYP2D6 enzyme but other compounds are able to inhibit the enzyme. The Plasma Protein Binding (PPB) model predicts whether a compound is likely to be highly bound to a carrier protein in the blood. Compound **6d**, **6e,** and **6j** bind at a level of less than 90% having AlogP98 less than 4.0, other compounds have binding >90%, clearly suggesting that have good bioavailability and are not likely to be high binding to carrier proteins in the blood.

The DruliTo software was used to obtain new drug-like leads generated hits were subjected to Lipinski's Rule of Five.[41] As per Lipinski's rule-of-five, an orally administrated drug should have log P ≤5, molecular weight (MW) <500 Daltons, hydrogen bond donor (HBD) ≤5, and hydrogen bond acceptor (HBA) ≤10. All the compounds have Lipinski's violation of molecular weight as shown in **Table 6**. Lipophilicity is a property that has a major effect both on the absorption, distribution, metabolism, excretion and toxicity properties, and pharmacological activity since many drugs cross biological membranes through passive transport, which strongly depends on their lipophilicity. Lipophilicity has been studied and applied as an important drug property for eras. Compounds **6d** showed the lowest lipophilicity, while compounds **6an** demonstrated the highest. It was found that all the ligands followed the Lipinski rule with maximum ligands (except **6d**, **6e**, **6j**, **6k**, **6o**, **6ad**, **6ae**, **6aj**, **6ak,** and **6ao**) showed no violation of the above criteria. Therefore, these ligands have good potential for ensuring development as an oral agent and can be potentially active drug candidates. The number of hydrogen bond acceptor value was beyond the Lipinski limit in case some compounds have not affected the bioactivity of the synthesized hybrids but they are highly effective against MTB.

3.4. Molecular docking study

In order to gain insight into the plausible mechanism of action of compounds docking simulations were performed. *In silico* docking studies were carried out with crystal structure of isoniazid-resistant I21V enoyl-ACP(COA) reductase mutant enzyme From *Mycobacterium tuberculosis* in Complex with NADH-INH (PDB entry: 2IE0) with native ligand isonicotinic-acetyl-nicotinamide-adenine dinucleotide (ZID) (Fig. 4 (a)). All the synthesized compounds were docked into active sites of isoniazid-resistant I21V enoyl-ACP(COA) reductase mutant enzyme has been reported as the target receptors for docking studies in finding the suitable drug candidates against the bacteria. A prerequisite to any successful experiment is the validation step. The validation of the docking procedure was performed by re-docking co-crystallized native ligand (ZID) into the active site of 2IE0 using YASARA software. In this analysis, the re-docked 2IE0 reproduced the binding pose with binding energy 11.4310 kcal/mol was found in Fig. 4 (c). which shows hydrogen bonding interactions, hydrophobic interaction, Van der Waals interactions, and π-π interactions were observed with peptides like Gly14, Ile16, Ser20, Val21, Ala22, Phe41, Leu63, Asp64, Val65, Gln66, Ser94, Ile95, Gly96, Phe97, Met98, Ile122, Ser123, Met147, Asp 148, Phe149, Tyr158, Met161, Lys165, Ala191, Gly192, Pro193, Thr196, Leu197, Ala198, Met199, and Leu218 were found as responsible key residues. The docked position was compared to the crystal structure position by calculating RMSD values 0.52 Å (Fig. 4 (d)). In general, RMSD values smaller than 2.0 Å indicates that the docking protocol is capable of accurately predicting the binding orientation of the co-crystallized ligand. In this study, RMSD values were within 2.0 Å, indicating our docking methods are validated for the given structures and YASARA software, therefore deemed reliable for docking of isoniazid-spirooxindole derivatives **(6a-6ao)** into the inhibitor binding cavity of 2IE0. The stereochemistry was measured of protein 2IE0 using the Ramachandran plot [42] implemented in RAMPAGE [43] (RAMPAGE server) exhibited 92.9% in ψ-ϕ core areas (Fig. 4 (b)). The occupancy of residues in most favored, additional allowed, and generally allowed regions with an exception of seven amino acids excluding general, Gly and Proline occupied in disallowed regions.

As it was possible to observe, all isoniazid-spirooxindole derivatives **(6a-6ao)** were docked into the defined binding pocket with the given docking input constraints. The best-docked poses were chosen on the basis of scoring function and their binding characteristics comparing with the reference ligand. Simplifying the docking result for compound **6m**, we described here the interaction map in Fig. 5 with the highest energy 12.6080 Kcal/mol. The nitro group of compound **6m** showed H-bonding with amino acids Phe41 (2.89 Å). The nitrogen of the pyridine ring shows H-bonding with amino acid Ile194 (3.10 Å). In addition, Van der Waals contacts and weak π-alkyl, π-sigma and other interactions were observed with peptides like Gly14, Ile15, Ile16, Thr17, Ser20, Val21, Ala22, Thr39, Gly40, Phe41, Ile47, Ser94, Ile95, Gly96, Phe97, Met103, Ile122, Met147, Phe149, Tyr158, Met161, Lys165, Pro193, Ile194, Thr196, Leu197, Ala198, and Met199. In contrast, Compound **6ao** has possessed the lowest binding energy of 11.0700 Kcal/mol. Similarly, the other representative compound **6ab** (Fig. 6) which showed the highest MIC value binds via two crucial H-bond strongly with Gly96 (1.83 & 1.91 Å) through -NH and -CO of the side chain. The nitrogen of the pyridine ring shows three H-

bonding with aminoacids Ile16 (4.69 Å), Leu197 (5.35 Å), and Ala198 (3.80 Å). The compound **6ab** was observed to be stabilized within the active site through strong van der Waals interactions, electrostatic interactions, weak π-alkyl, π-sigma and other interactions observed with residues Gly14, Ile16, Thr17, Ser19, Ser20, Phe41, Asp42, Arg43, Ser94, Ile95, Gly96, Phe97, Met98, Met103, Ile122, Thr196, Leu197, Ala198, Ile202, and Leu207. The π stacking was observed with Phe97 at an angle of 70.73 (5.03 and 4.60 Å) (Fig. 6). The amino acid Gly96 formed H-bond with -NH of isoniazid in compounds **6ab**, **6ad**, **6ae**, **6af**, **6ag**, **6ah**, **6aj**, **6ak**, **6al**, **6am**, **6an**, **6ao** at a distance of 3.03, 3.16, 2.82, 3.05, 3.22, 3.26, 3.21, 3.14, 3.14, 3.12, 3.00 and 2.92 Å, respectively. The information from the docking studies and In vitro anti-tubercular activity proved the newly synthesized compounds as potent towards the bacterial pathogens.

3.5. Molecular Dynamics simulations

Molecular dynamics simulations were used to study the binding affinity of selected ligands, in coherence with conformational changes of the isoniazid-resistant enoyl-ACP (COA) reductase-**6m** compound complex and the isoniazid-resistant enoyl-ACP (COA) reductase-**6ab** compound complex. This simulation study was executed at the physiological condition to account for the following strategies. The binding affinity of the selected ligands was obtained by docking experiments after that the molecular dynamics were performed on the target Isoniazid-resistant enoyl-ACP (COA) reductase-**6m** compound complex through the 10 ns production time to measure the binding stability of the ligand (Fig. 7). Energy and RMSD is an average taken over the residue given time scale. The average energy of the protein-ligand complex calculated over the simulation trajectory showed that (2IE0) developed effective interactions with the complete ligand dataset as their energies were in the range of -592099.596 kJ mol^{-1} to -777052.693 kJ mol^{-1} (Fig. 7). Various energy results were measured during molecular dynamics simulations, -777052.693 kJ mol^{-1} retrieved at the initial start while -592099.596 kJ mol^{-1} at 10 ns time trajectory and the average of energy has been recognized with -594320.779 kJ mol^{-1}. Different types of interactions were formed after the end of the dynamics simulation.

The simulation analyzed from the initial (0 ps) and final (10 ns) conformations, RMSD of common target trajectories highlighted the importance of H bonds and hydrophobic interactions conferred by hot spot residues. The protein-ligand interaction maps generated using protein-ligand interaction profiler showed that the dominance of the residue Phe41 and Phe149 exhibited less structural motions and acted as anchoring sites for ligand binding at the initial level of dynamics simulation. The diverse pattern of H-bonding with main and side chains of experimental hot spot residues (Ile16, Val21, Phe41, Val65, Ile95, Phe97, Ile122, Ile194, Met147, Leu197, Ala198,) was obtained after the completion of the 10 ns target trajectories. The corresponding RMSD values for the Gly96 residue represent large fluctuations with more than 2 Å and may act as ligand binding determinants. The isoniazid-resistant Enoyl-ACP (COA) reductase-**6m** compound-complex was used in receptor-based superposition to study the ensemble of simulation poses which shows the diverse pattern of the ligand interacted with the selected receptor (Fig. 8).

When we have performed molecular dynamics study using potent and hit biological active compound **6ab** with Isoniazid-resistant enoyl-ACP (COA) reductase protein through the 10 ns production time for conformational changes and binding stability of the ligand (Fig. 9-10). -763265.702 kJ mol^{-1} energy observed at the initial stage (0 ns) and -581658.933 kJ mol^{-1} at 10 ns time trajectory during the molecular dynamics simulations. The average energy has been documented -583951.885 kJ mol^{-1} during the entire MD of protein-**6ab**. An overall interaction diagram of protein residues, energy, and RMSD variation during molecular dynamic simulations is illustrated in Fig. 9-10.

4. Conclusion

Many antimycobacterial agents are available, still with limitations with respect to their activity due to increasing reports of multi-drug resistance. Hence, research on novel anti-TB drug agents is now intensively pursued to identify molecular targets and their modes of action. The present study involved the synthesis of a novel series of *N*'-(2-oxo-2-(2'-oxo-2-phenyl-1,10b-dihydrospiro[benzo[e]pyrazolo[1,5-c][1,3]oxazine-5,3'-indolin]-1'-yl)ethyl)isonicotinohydrazide derivatives. The novelty of these compounds is the most biologically active spirooxindole scaffold is to be linkage with very well-known tuberculosis drug isoniazid for the purpose of increasing activity. These new chemical entities displayed significant *in vitro* antimycobacterial activity against *Mycobacterium tuberculosis* $H_{37}Rv$ with the comparison of first-line drug isoniazid. Among them, compound **6ab** was found to be an active antimycobacterial agent. Further, the same compound **6ab** showed excellent MDR-TB activity out of some selected compounds. Additionally, all compounds were docked into the binding pocket of Isoniazid-resistant I21V Enoyl-ACP(COA) reductase mutant enzyme from *Mycobacterium tuberculosis* (PDB entry: 2IE0). Compound **6m** bind with highest energy 12.6080 Kcal/mol and of course, compound **6ab** also showed good binding with protein, in spite of showing only one violation of Lipinski's rule. Compound **6m** was analyzed for the molecular dynamics on the target Isoniazid-resistant Enoyl-ACP (COA) reductase-**6m** compound complex through the 10 ns production time to measure the binding stability of the ligand. Biological activity and molecular docking observations conclude that compounds **6ab** and **6m** would help in designing new strategies for the development of novel therapeutics, or improvement of existing pharmacotherapies against tuberculosis, a major burden for global health.

Acknowledgment

The authors are thankful to UGC-Info net and INFLIBNET Gujarat University for providing e-source facilities. The authors are thankful to the department of chemistry, Gujarat University for providing necessary facilities. The authors (M.N.B) and (M.A.B) are thankful to the UGC-BSR fellowship for financial support. Author is also very thankful to Edwin. A. Pithawala for biological activity support for this research work.

Supplementary data

Supplementary data associated with this article can be found, in the online version.

Author Contributions

The manuscript was written through the contributions of all authors. All authors have given approval to the final version of the manuscript.

Declaration of interests

The authors declare that they have no known competing financial interests or personal relationships that could have appeared to influence the work reported in this paper. The authors declare the following financial interests/personal relationships which may be considered as potential competing interests:

The authors have declared that there is not any conflict of interest.

5. References

[1] K. J. Ryan, C. G. Ray, Medical microbiology, McGraw Hill, 2004.

[2] E. W. Tiemersma, M. J. van der Werf, M. W. Borgdorff, B. G. Williams, N. J. Nagelkerke, Natural history of tuberculosis: duration and fatality of untreated pulmonary tuberculosis in HIV negative patients: a systematic review, PloS one 6 (2011) e17601.

[3] W. H. Organization, Global tuberculosis report 2015, 2015.

[4] M. Abdel-Aziz, H. M. Abdel-Rahman, Synthesis and anti-mycobacterial evaluation of some pyrazine-2-carboxylic acid hydrazide derivatives, Eur. J. Med. Chem. 45 (2010) 3384-3388.

[5] D. S. Rawat, Antituberculosis drug research: a critical overview, Med. Res. Rev. 33 (2013) 693-764.

[6] S. Gemma, L. Savini, M. Altarelli, P. Tripaldi, L. Chiasserini, S. S. Coccone, V. Kumar, C. Camodeca, G. Campiani, E. Novellino, Development of antitubercular compounds based on a 4-quinolylhydrazone scaffold. Further structure–activity relationship studies Bioorg. Med. Chem. 17 (2009)6063-6072.

[7] S. D Joshi, S. R Dixit, U. A More, T. Aminabhavi, V. H Kulkarni, A. K Gadad, Enoyl ACP reductase as effective target for the synthesized novel antitubercular drugs: a-state-of-the-art, Mini. Rev. Med. Chem. 14 (2014) 678-693.

[8] S. K. Jain, G. Lamichhane, S. Nimmagadda, M. G. Pomper, W. R. Bishai, Antibiotic treatment of tuberculosis: old problems, new solutions. Microbe-American Society For Microbiology 3 (2008) 285.

[9] P. Ahirrao, Recent developments in antitubercular drugs, Mini. Rev. Med. Chem. 8 (2008) 1441-1451.

[10] A. M. Ginsberg, Tuberculosis drug development: progress, challenges, and the road ahead, Tuberculosis 90 (2010) 162-167.

[11] A. Diacon, P. Donald, A. Pym, M. Grobusch, R. Patientia, R. Mahanyele, N. Bantubani, R. Narasimooloo, T. De Marez, R. Van Heeswijk, Randomized pilot trial of eight weeks of bedaquiline (TMC207) treatment for multidrug-resistant tuberculosis: long-term outcome, tolerability, and effect on emergence of drug resistance, Antimicrob. Agents Chemother. 56 (2012) 3271-3276.

[12] D. J. Knowles, antibacterial drug design, 1997.
[13] C. R. Harris, A. Thorarensen, Advances in the discovery of novel antibacterial agents during the year 2002, Curr. Med. Chem. 11 (2004) 2213-2243.
[14] H. A. Offe, W. Siefken, G. Domagk, Neoteben, ein neues, hochwirksames Tuberculostaticum und die Beziehungen zwischen Konstitution und tuberculostatischer Wirksamkeit von Hydrazinderivaten. Naturwissenschaften 39 (1952) 118-118.
[15] X. Zhao, H. Yu, S. Yu, F. Wang, J. C. Sacchettini, R. S. Magliozzo, Hydrogen peroxide-mediated isoniazid activation catalyzed by Mycobacterium tuberculosis catalase-peroxidase (KatG) and its S315T mutant. Biochemistry 45 (2006) 4131-4140.
[16] R. Rawat, A. Whitty, P. J. Tonge, The isoniazid-NAD adduct is a slow, tight-binding inhibitor of InhA, the Mycobacterium tuberculosis enoyl reductase: adduct affinity and drug resistance, Proc. Natl. Acad. Sci. 100 (2003) 13881-13886.
[17] T. C. Sarich, M. Youssefi, T. Zhou, S. P. Adams, R. A. Wall, J. M. Wright, Role of hydrazine in the mechanism of isoniazid hepatotoxicity in rabbits, Arch. Toxicol. 70 (1996) 835-840.
[18] G. Jin, D. Lu, S. Yao, C. C. Wu, J. X. Liu, D. A. Carson, H. B. Cottam, Amide derivatives of ethacrynic acid: synthesis and evaluation as antagonists of Wnt/β-catenin signaling and CLL cell survival, Bioorg. Med. Chem. Lett. 19 (2009) 606-609.
[19] S. Fortin, E. Moreau, J. Lacroix, M.-F. Côté, É. Petitclerc, C. René, Synthesis, antiproliferative activity evaluation and structure–activity relationships of novel aromatic urea and amide analogues of N-phenyl-N′-(2-chloroethyl) ureas, Eur. J. Med. Chem. 45 (2010) 2928-2937.
[20] M. A. Borad, M. N. Bhoi, N. P. Prajapati, H. D. Patel, Review of synthesis of spiro heterocyclic compounds from isatin, Synth. Commun. 44 (2014) 897-922.
[21] M. A. Borad, M. N. Bhoi, N. P. Prajapati, H. D. Patel, Review of synthesis of multispiro heterocyclic compounds from isatin, Synth. Commun. 44 (2014) 1043-1057.
[22] K. C. Joshi, P. Chand, Biologically active indole derivatives. Die Pharmazie 37 (1982) 1-12.
[23] V. V. Vintonyak, K. Warburg, H. Kruse, S. Grimme, K. Hübel, D. Rauh, H. Waldmann, Identification of thiazolidinones spiro- fused to indolin- 2- ones as potent and selective inhibitors of the mycobacterium tuberculosis protein tyrosine phosphatase B, Angew. Chem. Int. Ed. 49 (2010) 5902-5905.
[24] A. I. Almansour, S. Ali, M. A. Ali, R. Ismail, T. S. Choon, V. Sellappan, K. keyan Elumalai, S. Pandian, A regio-and stereoselective 1, 3-dipolar cycloaddition for the synthesis of new-fangled dispiropyrrolothiazoles as antimycobacterial agents, Bioorg. Med. Chem. Lett. 22 (2012) 7418-7421.
[25] M. A. Borad, M. N. Bhoi, D. P. Rajani, S. D. Rajani, H. D. Patel, synthesis and antimicrobial activities of 2-(4-substituted phenyl)-1, 10b dihydrospiro [benzo [e] pyrazolo [1, 5-c][1, 3] oxaz ine-5, 3’-indolin]-2'-one derivative from isatin. WJPPS. 3 (2014) 805-821.

[26] G. Canetti, W. Fox, A. a. Khomenko, H. Mahler, N. Menon, D. Mitchison, N. Rist, N. Šmelev, Advances in techniques of testing mycobacterial drug sensitivity, and the use of sensitivity tests in tuberculosis control programmes, Bull. World Health Organ. 41 (1969) 21.

[27] P. Kent, G. Kubica, Antituberculosis chemotherapy and drug susceptibility testing. Kent PT, Kubica GP. Public health mycobacteriology: a guide for the level III laboratory. Atlanta, GA: Centers for Disease Control and Prevention, (1985) 159-184.

[28] P. Anargyros, D. Astill, I. Lim, Comparison of improved BACTEC and Lowenstein-Jensen media for culture of mycobacteria from clinical specimens, J. Clin. Microbiol. 28 (1990) 1288-1291.

[29] R. Shah, R. Mehta, A. Parikh, Studies on Isoniazide Derivatives. Preparation and Antimicrobial Activity of 2- Aryl- 3- (pyridylcarbonyl)- 5- carboxymethyl- 4- thiazolidinones. Chemischer Informationsdienst 17 (1986).

[30] A. Cheng, K. M. Merz, Prediction of aqueous solubility of a diverse set of compounds using quantitative structure-property relationships., J. Med. Chem. 46, (2003) 3572-3580.

[31] W. J. Egan, G. Lauri, Prediction of intestinal permeability, Adv. Drug Deliv. Rev. 54 (2002) 273-289.

[32] S. L. Dixon, K. M. Merz, One-dimensional molecular representations and similarity calculations: methodology and validation, J. Med. Chem. 44 (2001) 3795-3809.

[33] R. G. Susnow, S. L. Dixon, Use of robust classification techniques for the prediction of human cytochrome P450 2D6 inhibition, J. Chem. Inf. Model. 43 (2003) 1308-1315.

[34] A. Cheng, S. L. Dixon, In silico models for the prediction of dose-dependent human hepatotoxicity, J. Comput. Aided Mol. Des. 17 (2003) 811-823.

[35] O. Trott, A. J. Olson, AutoDock Vina: improving the speed and accuracy of docking with a new scoring function, efficient optimization, and multithreading, J. Comput. Chem. 31 (2010) 455-461.

[36] E. Krieger, T. Darden, S. B. Nabuurs, A. Finkelstein, G. Vriend, Making optimal use of empirical energy functions: force- field parameterization in crystal space. Proteins: Structure, Function, and Bioinformatics 57 (2004) 678-683.

[37] M. V. B. Dias, I. B. Vasconcelos, A. M. X. Prado, V. Fadel, L. A. Basso, W. F. De Azevedo, D. S. Santos, Crystallographic studies on the binding of isonicotinyl-NAD adduct to wild-type and isoniazid resistant 2-trans-enoyl-ACP (CoA) reductase from Mycobacterium tuberculosis, J. Struct. Biol. 159 (2007) 369-380.

[38] U. C. Singh, P. A. Kollman, An approach to computing electrostatic charges for molecules, J. Comput. chem. 5 (1984) 129-145.

[39] Y. Duan, C. Wu, S. Chowdhury, M. C. Lee, G. Xiong, W. Zhang, R. Yang, P. Cieplak, R. Luo, T. Lee, A point- charge force field for molecular mechanics simulations of proteins based on condensed- phase quantum mechanical calculations, J. Comput. chem. 24 (2003) 1999-2012.

[40] S.-H. Lu, J. W. Wu, H.-L. Liu, J.-H. Zhao, K.-T. Liu, C.-K. Chuang, H.-Y. Lin, W.-B. Tsai, Y. Ho, The discovery of potential acetylcholinesterase inhibitors: a combination of pharmacophore modeling, virtual screening, and molecular docking studies, J Biomed Sci 18 (2011) b22.
[41] C. A. Lipinski, Drug-like properties and the causes of poor solubility and poor permeability, J. Pharmacol. Toxicol. Methods. 44 (2000) 235-249.
[42] G. N. Ramachandran, Stereochemistry of polypeptide chain configurations. *J. Mol. Biol.* 7 (1963) 95-99.
[43] RAMPAGE Server. Available at: http://ravenbioccam.ac.uk/ rampage.php, Accessed May (2014).

Abbreviations

ADMET	Absorption, distribution, metabolism, elimination, and toxicity
BBB	blood brain barrier
CADD	computer-aided drug design
FAS	Fatty Acid Synthase
FDA	Food and Drug Administration
INH	Isoniazid
MD	Molecular dynamics
MDR	Multi-drug-resistant
MIC	Minimum inhibitory concentration
MTB	Mycobacterium tuberculosis
NMR	Nuclear magnetic resonance
PDB	Protein data bank
PSA	Polar surface area
RMSD	Root mean squared deviation
RMSF	Root mean squared fluctuation
TB	Tuberculosis
TLC	Thin layer chromatography
WHO	World Health Organization
XDR	Extensively drug-resistant

YASARA Yet Another Scientific Artificial Reality Application

List of captions:

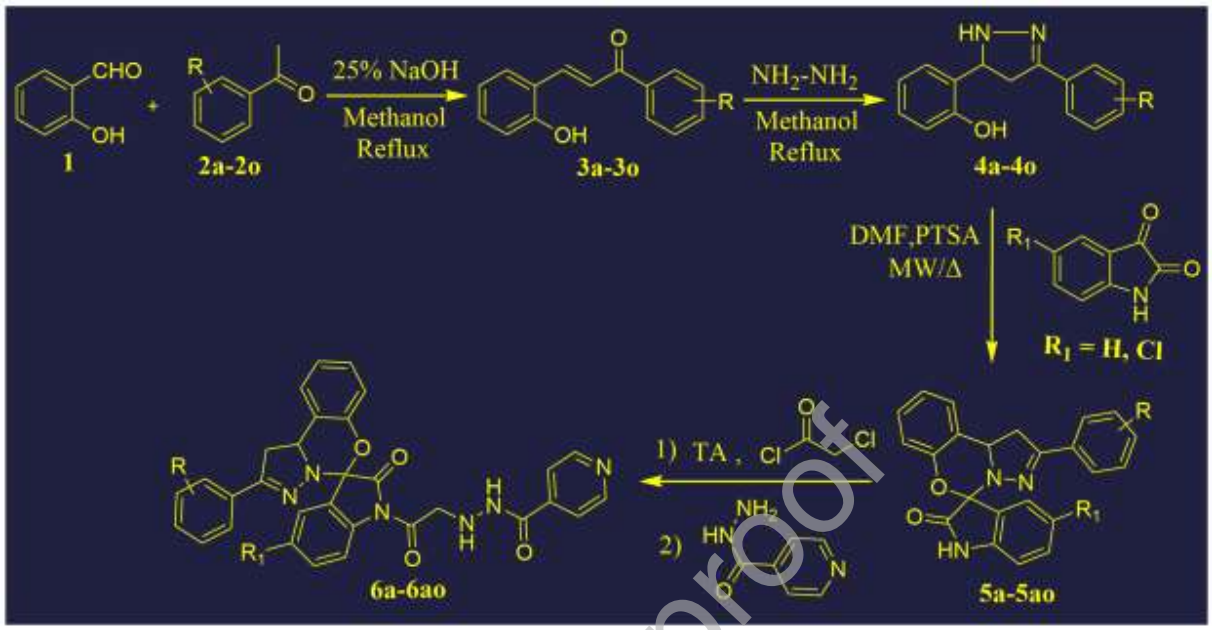

Scheme 1 Synthetic pathway for the synthesis of title compound **6a-6ao**

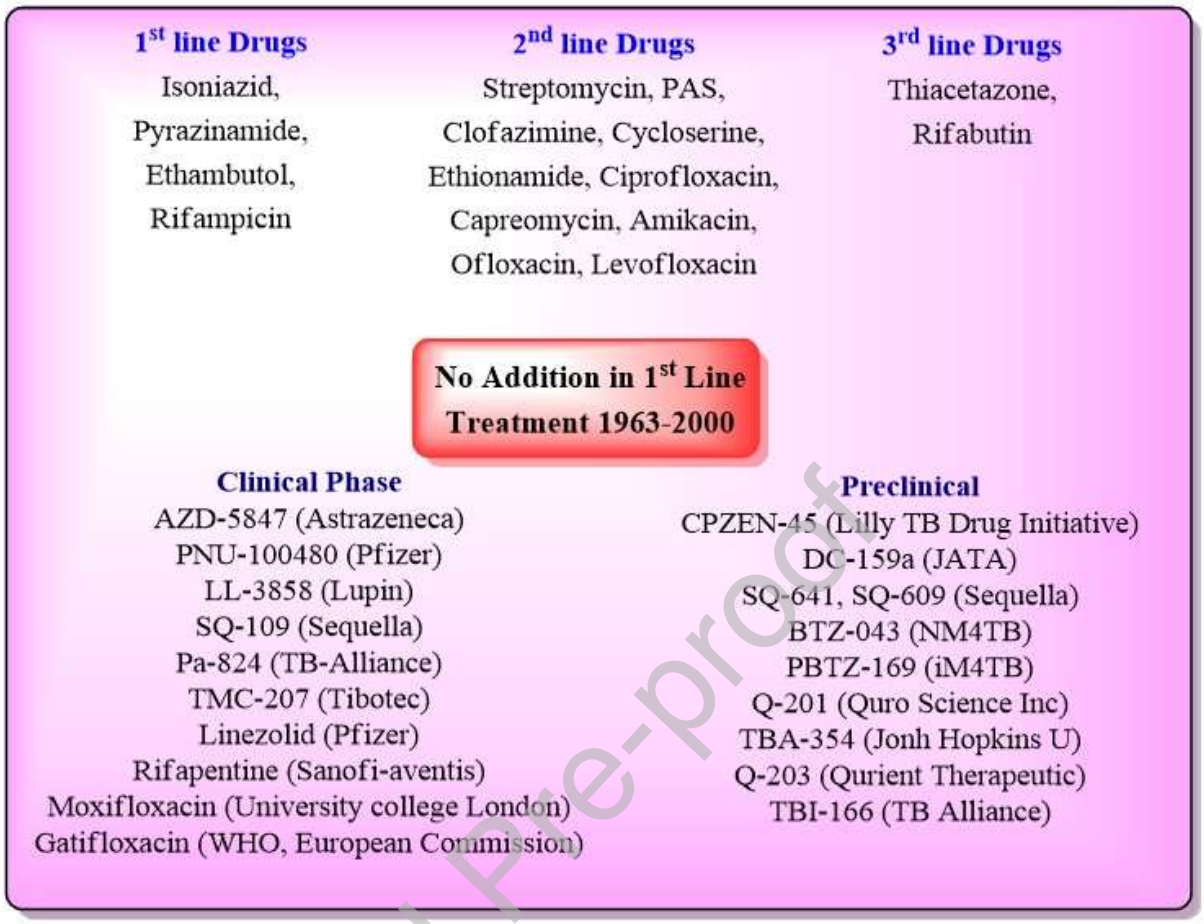

Figure 1 Drug discovery in TB

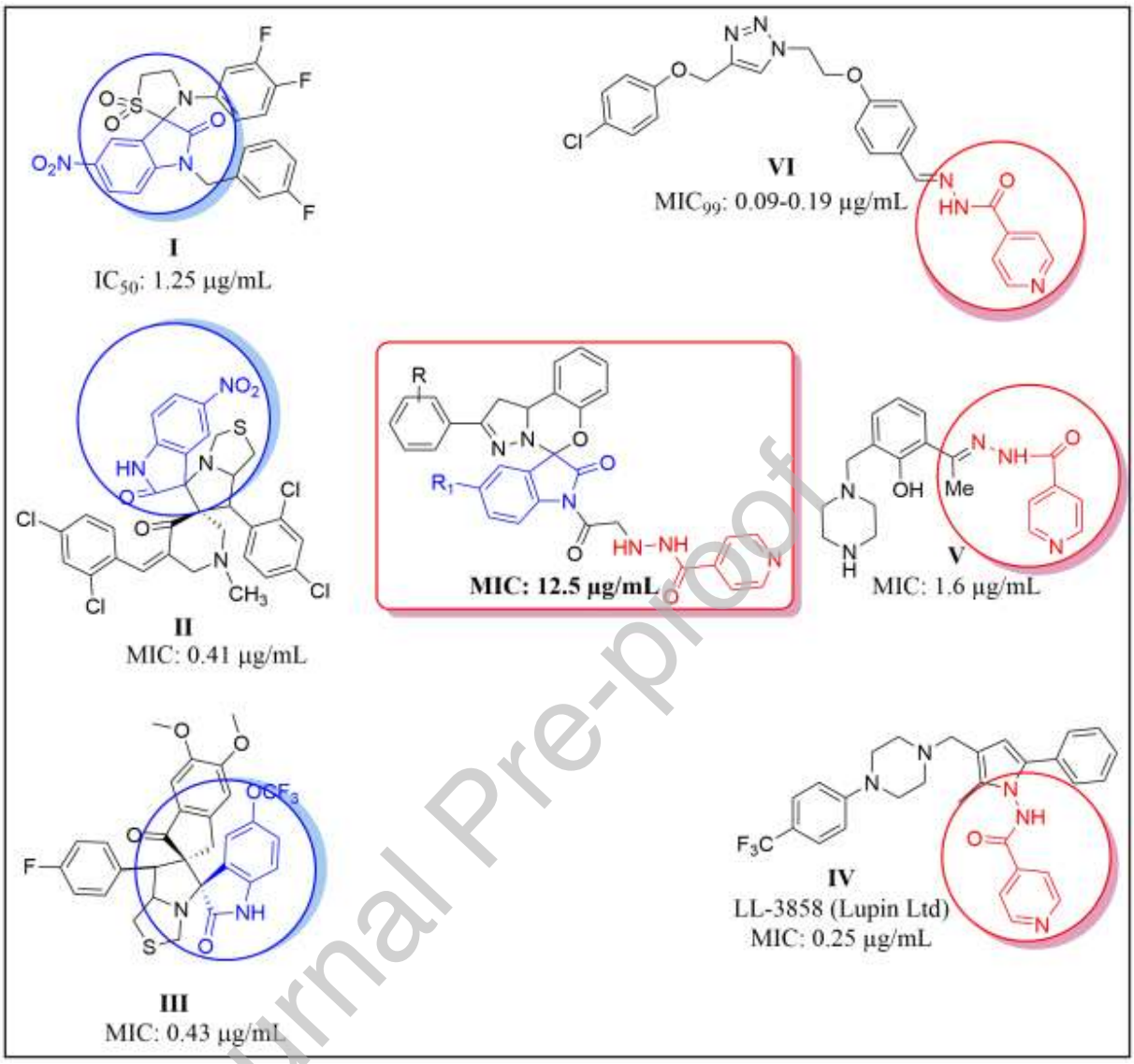

Figure 2 Some of the structures as representative antimycobacterial agents containing spirooxindole scaffold and isoniazid for designing of compounds

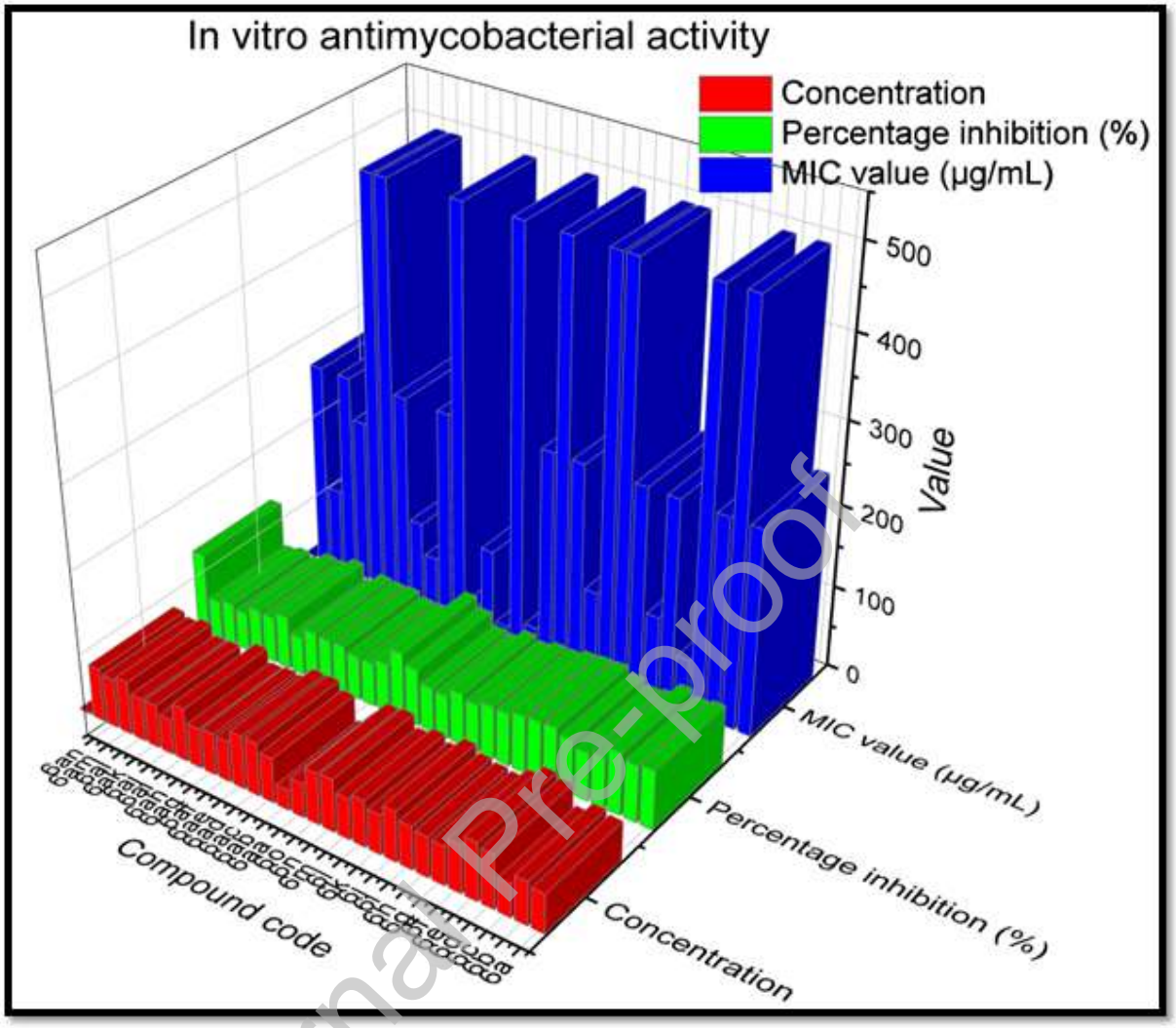

Figure 3 Graphical representation of in vitro antimycobacterial activity of synthesized compounds (**6a-6ao**)

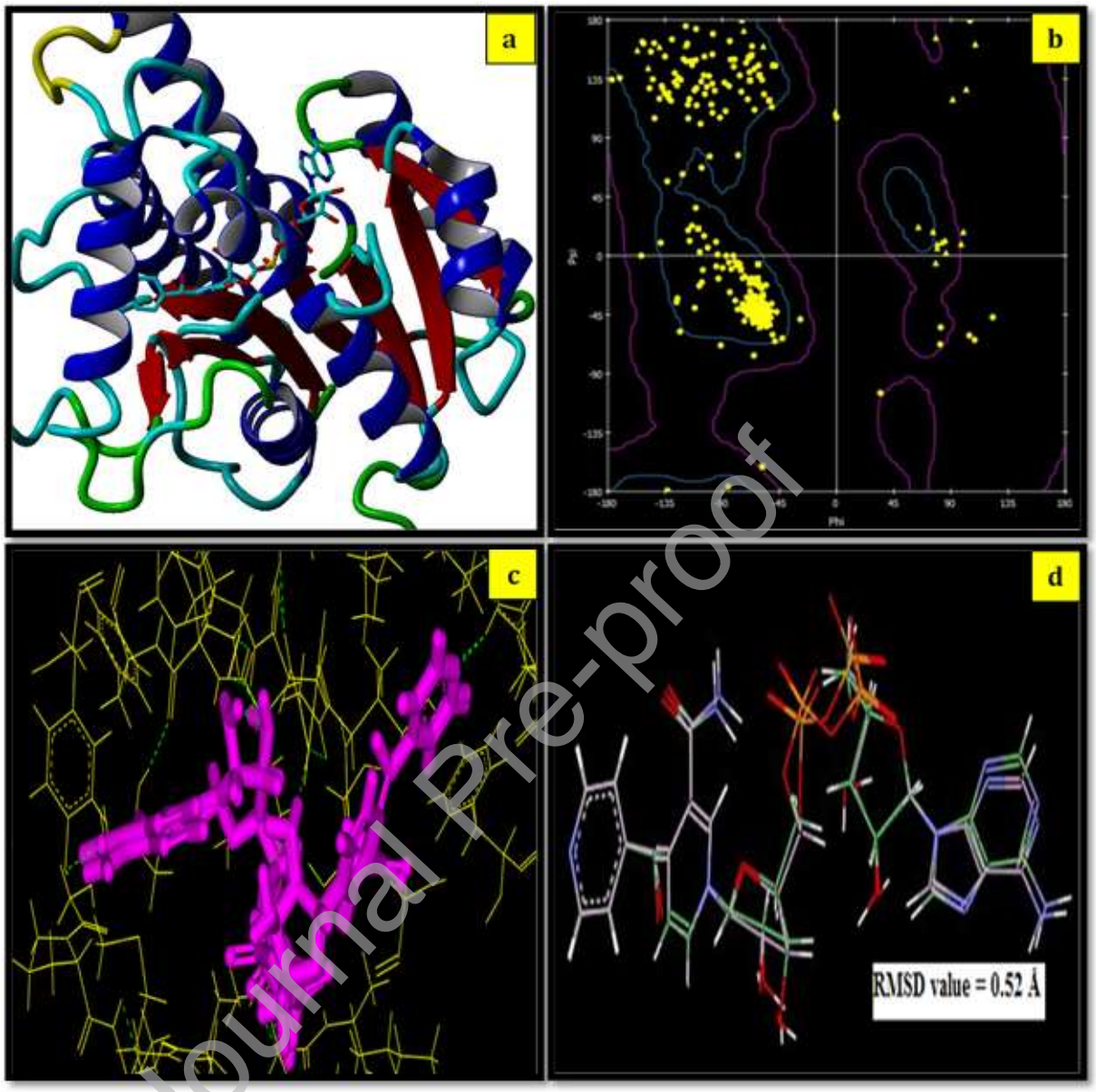

Figure 4 (a) Crystal structure of Isoniazid-resistant I21V Enoyl-ACP(COA) Reductase in Complex with NADH-INH (PDB entry: 2IE0) **(b)** Ramachandran plot of 2IE0 showed 92.9% in core regions **(c)** Native co-crystallized ligand isonicotinic-acetyl-nicotinamide-adenine dinucleotide (ZID) docked within the active site of 2IE0. **(d)** Superimposition of native ligand and reference ligand exhibiting RMSD values 0.52 Å

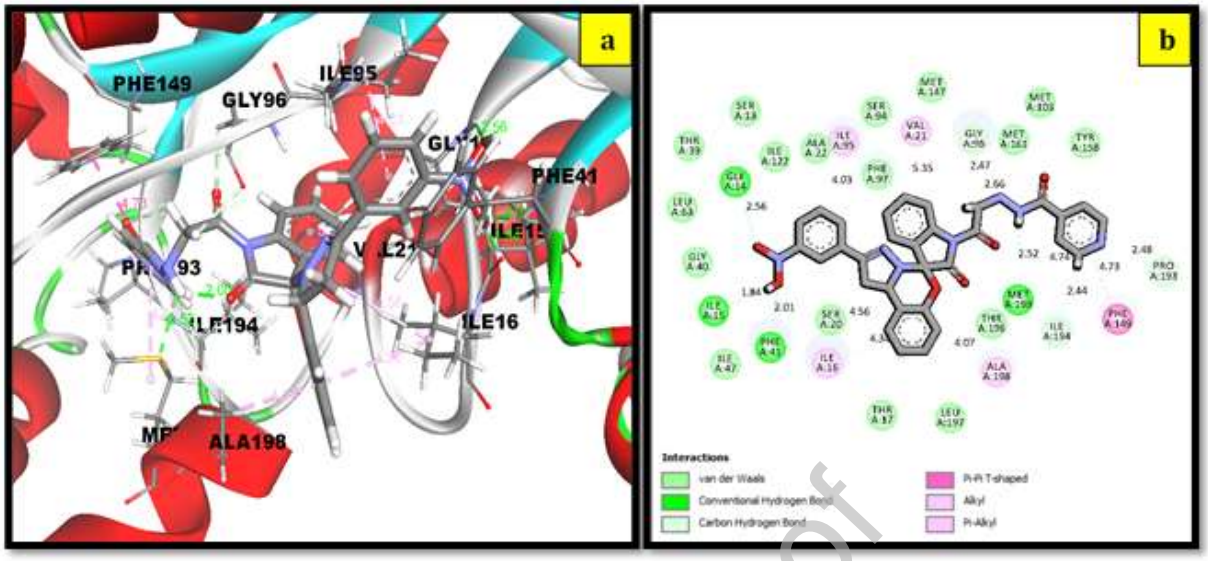

Figure 5 (a) Docked pose of compound **6m** into the binding site of 2IE0. **(b)** The 2D orientation of the ligand **6m** into the binding pocket of the 2IE0 protein

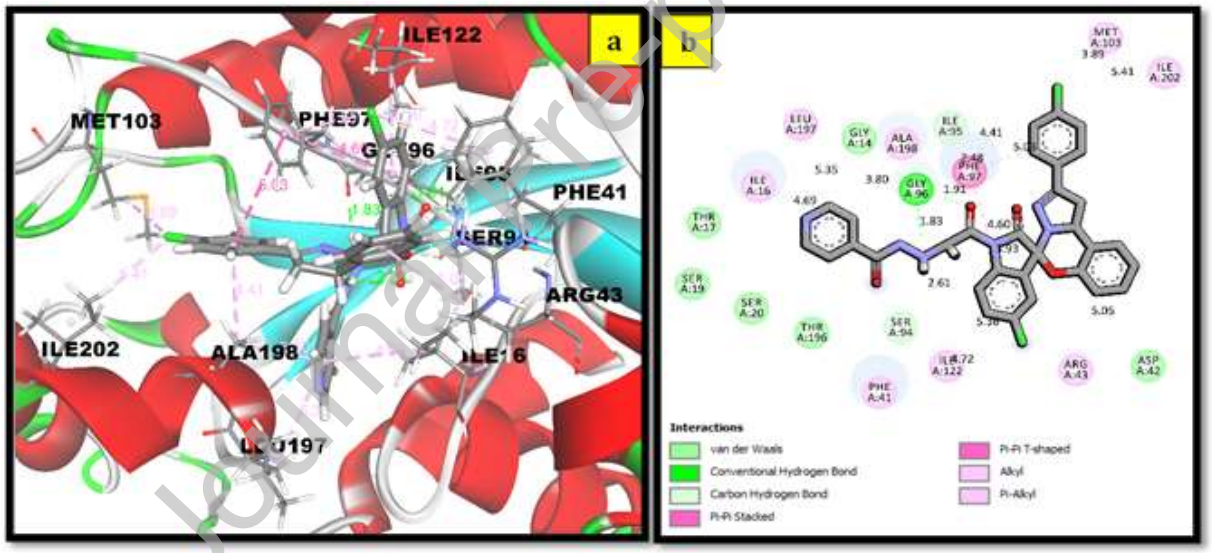

Figure 6 (a) Docked pose of compound **6ab** into the binding site of 2IE0. **(b)** The 2D orientation of the ligand **6ab** into the binding pocket of the 2IE0 protein

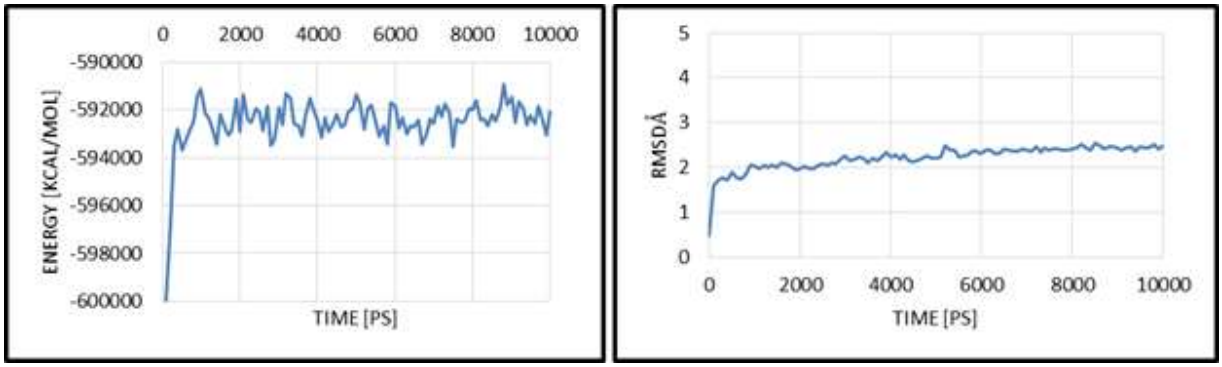

Figure 7 Energy plot and RMSD plot Produced from MD Trajectories of Prioritized Target: isoniazid-resistant Enoyl-ACP (COA) Reductase-Compound 6m Complex

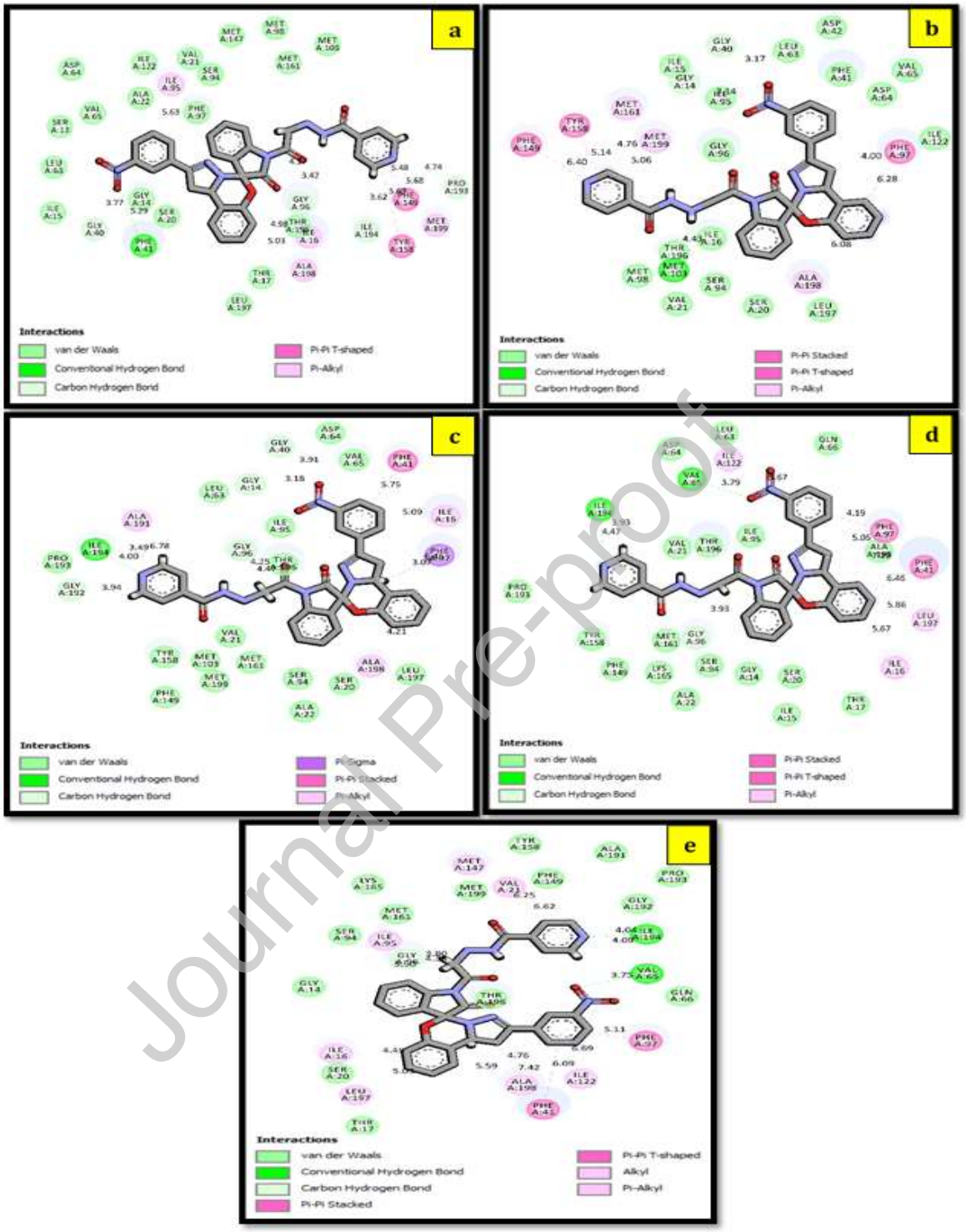

Figure 8 The protein-ligand interaction maps developed from 0 ns to 10 ns (a-e) of molecular dynamics (MD) conformations of prioritized Protein-6m

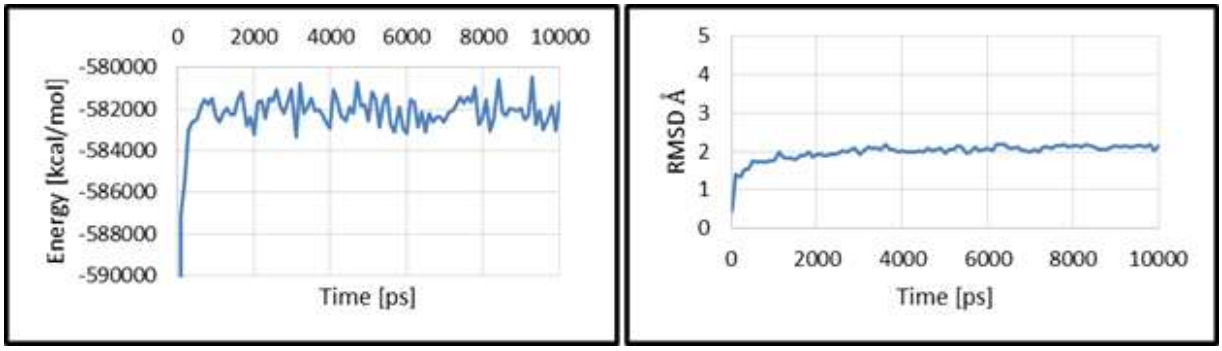

Figure 9 Energy Plot and RMSD Plot Produced from MD Trajectories of Prioritized Target: isoniazid-resistant Enoyl-ACP (COA) Reductase-Compound 6ab Complex

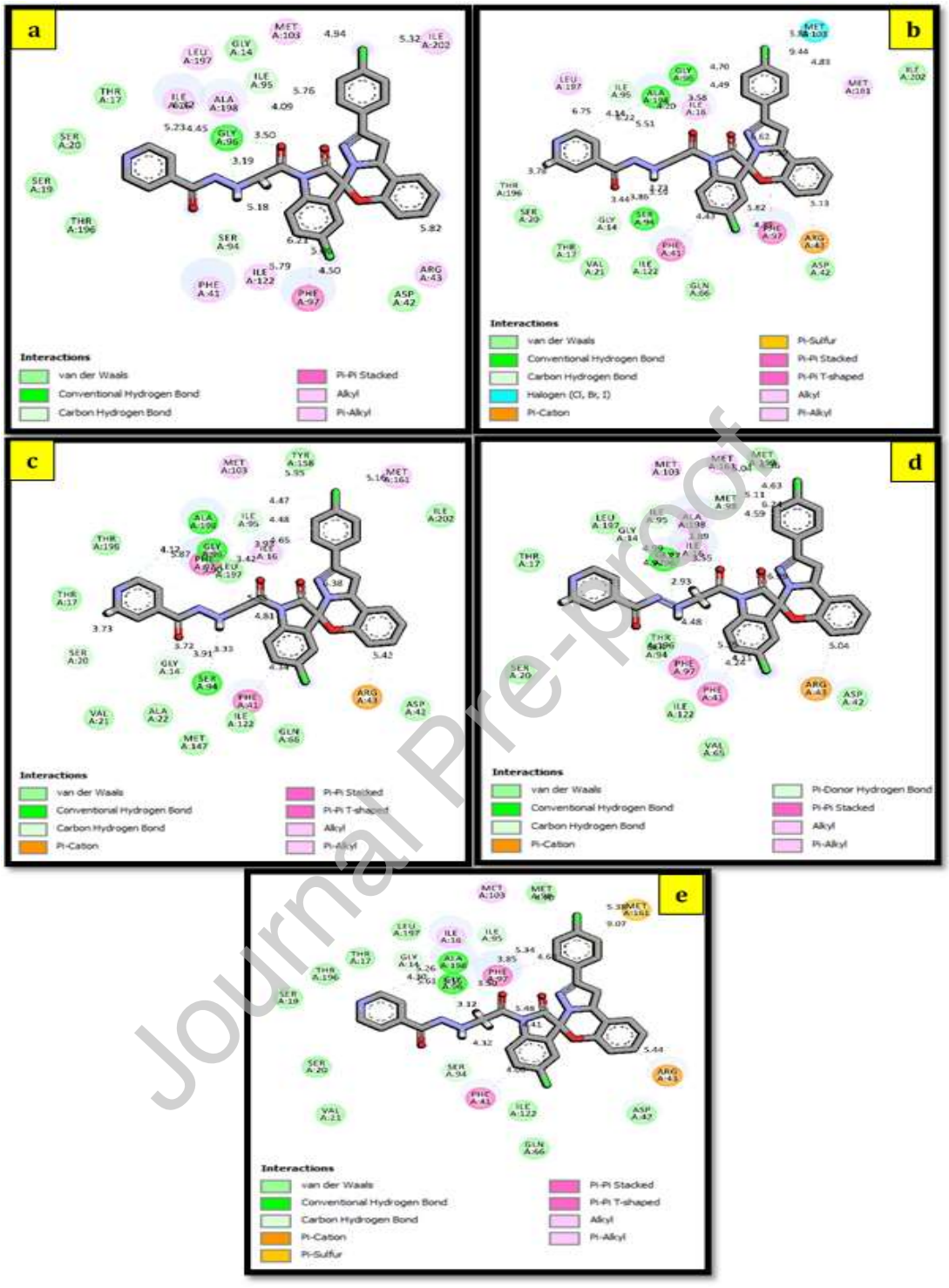

Figure 10 The protein-ligand interaction maps developed from 0 ns to 10 ns (a-e) of molecular dynamics (MD) conformations of prioritized Protein-6ab

CREDIT AUTHOR STATEMENT

Authorship contributions:

Conception and design of study: Mayuri A. Borad, Divya J. Jethava, Manoj N. Bhoi, Hitesh D. Patel

Acquisition of data: Mayuri A. Borad, Divya J. Jethava, Manoj N. Bhoi,

Analysis and/or interpretation of data: Mayuri A. Borad, Divya J. Jethava, Manoj N. Bhoi,

Computational work: Mayuri A. Borad, Divya J. Jethava, Manoj N. Bhoi, Chirag N. Patel, Himanshu A.
Pandya, Hitesh D. Patel

Drafting the manuscript: Mayuri A. Borad, Divya J. Jethava, Manoj N. Bhoi, Hitesh D. Patel

Revising the manuscript critically for important intellectual content: Mayuri A. Borad, Divya J.
Jethava, Manoj N. Bhoi, Hitesh D. Patel

Table 1 ADMET descriptors and their rules/keys

	HIA[a]				**solubility**						**BBB[b]**				**CYP2 D6[c]**		**Hepa totox icity[d]**		**PPB[e]**		
Level	0	1	2	3	0	1	2	3	4	5	0	1	2	3	0	1	0	1	0	1	2
Description	Good absorption	Moderate absorption	Low absorption	Very low absorption	Extremely low	No, very low, but possible	Yes, low	Yes, good	Yes, optimal	No, too soluble	Very High	High	Medium	Low	Non inhibitor	Inhibitor	Nontoxic	Toxic	Binding is <90%	Binding is ≥90%	Binding is ≥95%

*a= human intestinal absorption, b= blood brain barrier, c=cytochrome P450 2D6 enzyme inhibition, d= human hepatotoxicity, e= plasma protein binding property

Table 2 Comparison of yield and melting point for the synthesis of 6a-6ao

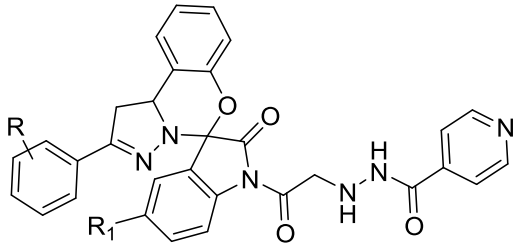

Entry	Product code	R	R_1	Yield (%)	mp °C
1	**6a**	4-H	H	65.84	150-152
2	**6b**	4-Cl	H	62.15	133-130
3	**6c**	4-Br	H	71.28	193-192
4	**6d**	4-NH_2	H	79.51	120-121
5	**6e**	4-OH	H	63.22	163-162
6	**6f**	4-CH_3	H	67.49	122-120
7	**6g**	4-F	H	74.25	173-175
8	**6h**	3-Br	H	60.12	194-196
9	**6i**	4-NO_2	H	62.15	167-168
10	**6j**	2-OH	H	60.15	109-110
11	**6k**	4-OCH_3	H	75.45	184-186
12	**6l**	2-Cl	H	65.19	104-106
13	**6m**	3-NO_2	H	61.12	146-149
14	**6n**	2,4-di-Cl	H	60.56	189-190
15	**6o**	2-OCH_3	H	74.45	179-182
16	**6aa**	4-H	Cl	79.58	110-111
17	**6ab**	4-Cl	Cl	76.42	164-166
18	**6ac**	4-Br	Cl	79.16	144-145
19	**6ad**	4-NH_2	Cl	74.28	162-165
20	**6ae**	4-OH	Cl	62.25	126-128
21	**6af**	4-CH_3	Cl	77.18	171-172
22	**6ag**	4-F	Cl	63.45	196-198
23	**6ah**	3-Br	Cl	77.63	130-131
24	**6ai**	4-NO_2	Cl	62.45	150-152
25	**6aj**	2-OH	Cl	65.79	120-122
26	**6ak**	4-OCH_3	Cl	76.13	112-115
27	**6al**	2-Cl	Cl	74.88	122-123
28	**6am**	3-NO_2	Cl	78.15	159-162
29	**6an**	2,4-di-Cl	Cl	63.19	166-167
30	**6ao**	2-OCH_3	Cl	64.78	129-130

Table 3 *in vitro* antimycobacterial (MTB) screening of compound 6a-6ao

Compound code	Lowenstein–Jensen (L-J) method (Culture: $H_{37}Rv$)			MIC value (µg/mL)
	Mean Colony Forming Unit on media			
	Control	Treatment concentration* (1000 µg/ml) *Mean±S.E*	Percentage inhibition (%)	
6a	173	48±1.215	72.25	250
6b	173	53±1.256	69.36	500
6c	173	41±1.217	76.30	250
6d	173	66±1.259	61.84	500
6e	173	71±1.194	58.95	62.5
6f	173	59±1.219	65.89	250
6g	173	48±1.225	72.25	100
6h	173	50±1.195	71.09	250
6i	173	53±1.251	69.36	500
6j	173	62±1.234	64.16	500
6k	138	49±1.241	64.49	100
6l	138	57±1.218	58.69	250
6m	138	50±1.193	63.76	500
6n	138	65±1.261	52.89	250
6o	138	63±1.260	54.34	25
6aa	138	42±1.247	69.59	500
6ab	**138**	**25±1.246**	**81.88**	**12.5**
6ac	138	55±1.198	60.14	100
6ad	138	65±1.242	52.89	25
6ae	138	65±1.284	52.89	500
6af	121	50±1.260	58.67	250
6ag	121	51±1.248	57.85	62.5
6ah	121	49±1.270	59.50	100
6ai	121	65±1.194	46.28	250
6aj	121	43±1.247	64.46	500
6ak	121	53±1.283	56.19	500
6al	121	52±1.249	57.02	200
6am	121	65±1.281	46.28	250
6an	121	60±1.263	50.41	100
6ao	121	65±1.272	46.28	250
Isoniazid	173	02±1.225	98.84	0.20

* p value < 0.05, data significant.

Table 4 *in vitro* antimycobacterial (MDR-TB) screening

Lowenstein–Jensen (L-J) method (Culture: MDR)										
Compound code	**6a**	**6b**	**6e**	**6g**	**6h**	**6o**	**6ab**	**6ad**	**6ag**	**Kanamycin**
MIC value (µg/mL)	500	500	100	125	1000	62.5	**50**	62.5	500	62.5

Table 5 Calculated ADMET properties of compound 6a-6ao

Compound code	BBB level	HIA level	Solubility level	Hepato toxicity	CYP2D6	PPB level	AlogP98	PSA_2D
6a	4	1	1	1	1	2	4.1	115.74
6b	4	2	1	1	1	1	4.8	115.74
6c	4	2	1	1	1	1	4.8	115.74
6d	4	2	1	1	1	0	3.3	142.28
6e	4	2	2	1	1	0	3.9	136.55
6f	4	2	1	1	1	1	4.6	115.74
6g	4	1	1	1	1	1	4.3	115.74
6h	4	2	1	1	1	1	4.8	115.74
6i	4	3	1	1	1	1	4.0	158.56
6j	4	2	2	1	1	0	3.9	136.55
6k	4	2	2	1	1	1	4.1	124.67
6l	4	2	1	1	1	1	4.8	115.74
6m	4	3	1	1	0	1	4.0	158.56
6n	4	2	1	1	0	2	5.4	115.74
6o	4	2	1	1	1	1	4.1	124.67
6aa	4	2	1	1	1	1	4.8	115.74
6ab	4	2	1	1	1	2	5.4	115.74
6ac	4	2	1	1	1	2	5.5	115.74
6ad	4	2	1	1	1	1	4.0	142.28
6ae	4	2	1	1	1	1	4.5	136.55
6af	4	2	1	1	1	2	5.2	115.74
6ag	4	2	1	1	1	2	5.0	115.74
6ah	4	2	1	1	1	2	5.5	115.74
6ai	4	3	1	1	0	1	4.7	158.56
6aj	4	2	1	1	0	1	4.5	136.55
6ak	4	2	1	1	1	1	4.7	124.67
6al	4	2	1	1	0	2	5.4	115.74
6am	4	3	1	1	1	1	4.7	158.56
6an	4	2	0	1	0	2	6.1	115.74
6ao	4	2	1	1	1	1	4.7	124.67
isoniazid	3	0	4	0	0	1	-0.8	167.91

Table 6 Prediction of Lipinski's 'Rule of 5' for the compound 6a-6ao

Compound code	Molecular weight (<500)	Log P (≤5)	HBA (≤10)	HBD (≤5)	Lipinski violation
6a	544.57	1.294	10	2	1
6b	579.01	1.238	10	2	1
6c	623.47	1.414	10	2	1
6d	559.59	0.169	11	3	2
6e	560.57	0.580	11	3	2
6f	558.60	1.686	10	2	1
6g	562.56	0.777	10	2	1
6h	623.47	1.414	10	2	1
6i	589.57	0.878	10	2	1
6j	560.57	0.791	11	3	2
6k	574.60	0.901	11	2	2
6l	579.01	1.449	10	2	1
6m	589.57	0.878	10	2	1
6n	613.46	1.815	10	2	1
6o	574.60	1.112	11	2	2
6aa	579.01	1.660	10	2	1
6ab	613.46	1.604	10	2	1
6ac	657.91	1.780	10	2	1
6ad	597.03	0.535	11	3	2
6ae	595.01	0.946	11	3	2
6af	593.04	2.052	10	2	1
6ag	597.00	1.143	10	2	1
6ah	657.91	1.780	10	2	1
6ai	624.01	1.244	10	2	1
6aj	595.01	1.157	11	3	2
6ak	609.04	1.267	11	2	2
6al	613.46	1.815	10	2	1
6am	624.01	1.244	10	2	1
6an	647.90	2.181	10	2	1
6ao	609.04	1.478	11	2	2